



The Impact of a Simple Representation of Non-Structural Carbohydrates on the Simulated Response of Tropical Forests to Drought

Simon Jones¹, Lucy Rowland², Peter Cox¹, Debbie Hemming³, Andy Wiltshire³, Karina Williams^{3,4}, Nicolas C. Parazoo⁵, Junjie Liu⁵, Antonio C. L. da Costa⁶, Patrick Meir^{7,8}, Maurizio Mencuccini^{9,10}, and Anna Harper¹

¹College of Engineering, Mathematics and Physical Sciences, University of Exeter, Exeter, Devon EX4 4QF, UK

²College of Life and Environmental Sciences, University of Exeter, Exeter, Devon EX4 4QF, UK

³Met Office Hadley Centre, FitzRoy Road, Exeter EX1 3PB, UK

⁴Global Systems Institute, University of Exeter, Laver Building, North Park Road, Exeter EX4 4QE

⁵California Institute of Technology, Jet Propulsion Laboratory, 4800 Oak Grove Drive, Pasadena, CA 91109

⁶Instituto de Geosciencias, Universidade Federal do Para, Belem, Brazil

⁷Research School of Biology, Australian National University, Canberra ACT 2601 Australia and

⁸School of Geosciences, University of Edinburgh, Edinburgh EH9 3FF UK

⁹ICREA, Pg. Lluís Companys 23, 08010 Barcelona (Spain)

¹⁰CREAF, Universitat Autònoma de Barcelona, Cerdanyola del Valles 08193, Barcelona (Spain)

Correspondence: Simon Jones (sj326@exeter.ac.uk)

Abstract. Accurately representing the response of ecosystems to environmental change in land surface models (LSM) is crucial to making accurate predictions of future climate. Many LSMs do not correctly capture plant respiration and growth fluxes, particularly in response to extreme climatic events. This is in part due to the unrealistic assumption that total plant carbon expenditure (PCE) is always equal to gross carbon accumulation by photosynthesis. We present and evaluate a simple model of labile carbon storage and utilisation (SUGAR), designed to be integrated into an LSM, that allows simulated plant respiration and growth to vary independently of photosynthesis. SUGAR buffers simulated PCE against seasonal variation in photosynthesis, producing more constant (less variable) predictions of plant growth and respiration relative to an LSM that does not represent labile carbon storage. This allows the model to more accurately capture observed carbon fluxes at a large-scale drought experiment in a tropical moist forest in the Amazon, relative to the Joint UK Land Environment Simulator LSM (JULES). SUGAR is designed to improve the representation of carbon storage in LSMs and provides a simple framework that allows new processes to be integrated as the empirical understanding of carbon storage in plants improves. The study highlights the need for future research into carbon storage and allocation in plants, particularly in response to extreme climate events such as drought.

1 Introduction

Forests cover nearly 4000 Mha (UN Food and Agriculture Organization Rome, 2015) of the world's land surface and store roughly 850 Pg (861±66 Pg) of carbon (Pan et al., 2011). They represent a significant sink of carbon from the atmosphere,



sequestering $2.4 \pm 0.4 \text{ PgCyr}^{-1}$, roughly 25% of total annual anthropogenic carbon emissions (IPCC, 2014). The extent to which carbon uptake by forests will continue under future climate change is uncertain, as global climate models (GCM) disagree not only on the magnitude of future terrestrial carbon uptake, but also the sign (Cox et al., 2000; Sitch et al., 2008; Hewitt et al., 2016; Arora et al., 2013). Some models predict large increases in terrestrial carbon stocks by the end of the century, while others predict significant losses, with an uncertainty in projections of more than 160PgC by the year 2100 (Lovenduski and Bonan, 2017). Much of this uncertainty stems from deficiencies in the structure of the land surface model (LSM) component of GCMs and is exacerbated by positive feedback loops between the land and atmosphere (Lovenduski and Bonan, 2017; Huntingford et al., 2009, 2013; Friedlingstein et al., 2001) Significant improvements in LSMs are required to constrain model outputs and reduce uncertainty in future climate projections.

10

The carbon balance of forested ecosystems is dictated by the relative magnitudes of photosynthesis, plant growth and autotrophic respiration. Most LSMs simulate growth and respiration as equal to instantaneous photosynthesis (Fatichi et al., 2014). Consequently at any given time, the total rate of carbon utilisation by respiration and growth, referred to as plant carbon expenditure (PCE), is equal to the rate of carbon accumulation by photosynthesis, commonly referred to as gross primary productivity (GPP). However, in reality growth and respiration are not so strictly coupled to photosynthesis and plants regularly experience periods when the supply of carbon from photosynthesis does not equal the demands of growth and respiration (Körner, 2003; Muller et al., 2011). This asynchrony between supply and demand is facilitated by reserve pools of labile carbon known collectively as non-structural carbohydrates (NSCs). The NSC pool within a plant accumulates when photosynthesis exceeds carbon demand and is drawn upon to sustain growth and respiration when they are not supported by instantaneous photosynthetic assimilation (Hartmann and Trumbore, 2016; Dietze et al., 2014). NSCs therefore act as a buffer, allowing key functional processes to be maintained, even when photosynthetic accumulation is low. This buffering is particularly important during periods of environmental stress, which can lead to reduced productivity over seasonal to multi-annual time-scales. During prolonged periods of stress, carbon utilisation rates can diverge significantly from photosynthesis (Metcalf et al., 2010; Doughty et al., 2015b, a) and so plants rely heavily on their NSC reserves. Without simulating NSC storage LSMs remain unable to capture this asynchrony between GPP and PCE and so fail to correctly simulate forest level respiration and growth fluxes.

The ability to sustain respiration and growth during periods of reduced productivity is an important process that can allow plants to survive extreme short-term climate events, such as drought (Doughty et al., 2015b). Consequently, NSC dynamics are also inextricably linked to plant mortality. Under low water availability the transport of water from roots to other organs can be compromised by the cavitation of xylem in the plant (Martínez-Vilalta et al., 2014; Sperry and Love, 2015; Tyree and Sperry, 1989). Xylem damage can lead to a drop in hydraulic conductance, resulting in damage to plant tissue and increased risk of mortality (Rowland et al., 2015; Anderegg and Anderegg, 2013; McDowell et al., 2008) Plants combat this threat through control over the aperture of their stomata. Closing the stomata reduces water loss through transpiration and lowers the risk of xylem damage and hydraulic failure. The trade-off to this strategy is a reduction in productivity. The ability of a plant to employ this strategy is therefore reliant on its ability to store and utilise NSC. Recent developments in modelling plant hydraulics (Mencuccini et al., 2019; Eller et al., 2018; Sperry et al., 2017; Baker et al., 2008) provide more accurate predictions of stomatal behaviour during drought, however, these developments must also be accompanied by models of carbon storage in order to effectively simulate the trade-off between hydraulic damage and productivity loss. If carbon demand exceeds supply over long periods of drought, NSC reserves will become exhausted, causing essential elements of plant function to fail, a process termed 'carbon starvation'. Carbon starvation can also lead to increased mortality rates (Galiano et al., 2011; Adams et al., 2013) and so there is a complex balance between stomatal closure and NSC storage (Mitchell et al., 2013; Adams et al., 2017) that must be captured by LSMs in order to accurately capture climate driven mortality.

Accurately simulating forest mortality is vital to accurate predictions of climate. This is particularly true in tropical regions where terrestrial carbon storage is large (Pan et al., 2011) and forests are frequently subjected to intense periods of environmental stress. Intense dry periods can reduce vegetation productivity and increase plant mortality in the tropics, over both short-term (Phillips et al., 2009; Bastos et al., 2018; Luo et al., 2018; Gloor et al., 2018) and multi-annual time-scales (Rowland et al., 2015; Meir et al., 2018; Metcalfe et al., 2010; Fisher et al., 2007; da Costa et al., 2010). When combined with the effects of fire and land-use change, drought can cause regions such as the Amazon basin to shift from a net sink to a net source of carbon to the atmosphere (Gatti et al., 2014; Liu et al., 2017; Phillips et al., 2009). Loss of terrestrial carbon in the Amazon represents a significant feedback loop in the climate system (Cox et al., 2000) and large losses of biomass could cause drastic and irreversible changes to the climate. However, the nature of this 'tipping point' is uncertain, and without accurate representation of forest resilience, including the balance between hydraulic failure and carbon starvation, predictions of large-scale forest die-back will remain unreliable. Drought is predicted to increase in both frequency and severity across the

55



Simon Jones: A Simple Representation of NSC

3

tropical rainforest biome in response to climate change (Marengo et al., 2018; IPCC, 2014). Accurately simulating drought responses is, therefore, a priority for the global modelling community (Corlett, 2016; Fatichi et al., 2016), although many efforts to date have focused on simulating plant hydraulic properties and have largely ignored the development of a NSC pool in models.

Despite their clear role in forest function, our current understanding of how NSCs are produced, stored and used remains poor (Hartmann and Trumbore, 2016). Absolute pool sizes are difficult to quantify (Quentin et al., 2015) and it is not clear how NSC reserves are distributed and transported between different plant organs under stress (Martínez-Vilalta et al., 2016; Sevanto et al., 2014). It is also not clear whether NSC storage is the passive result of asynchrony between supply demand as described above, or whether plants also have the capacity to actively regulate NSC stores at the expense of growth and respiration (Körner, 2003; Palacio et al., 2014; Wiley and Helliker, 2012). This may go some way to explaining the apparent absence of substrate-based modelling approaches within many LSMs. Some optimised modelling studies have been conducted that explore models of NSC storage and the substrate limitation of respiration and growth (Thornley, 1970, 1971, 1972a, b, 1977, 1991, 1997, 2011; Thornley and Cannell, 2000; Dewar et al., 1999). These provide a theoretical framework to develop mechanistic models of NSC storage and utilisation (Hemming et al., 2001; Fritts et al., 2000; Salomón et al., 2019) that allow detailed simulations of plant function. However, there have been few attempts to develop such models in a manner that would be compatible with large scale LSMs (De Kauwe et al., 2014). This can largely be attributed to a scarcity of ecosystem level data (NSC content and distribution) that can be used to parametrise and evaluate models for a range of species and climates that covers all plant functional types (PFTs) used in LSMs (Fatichi et al., 2019). Given our current knowledge and data-availability it is necessary to develop a simplistic model that can be easily parametrised off data sources that can be more effectively collected (e.g. growth and respiration data), yet capture the essential characteristics of representing a NSC pool (e.g. de-coupling photosynthesis from growth and respiration). Such an effort will not only constrain future climate projections, but may also be used to stimulate further research that improves our empirical understanding of NSC storage and use.

In this study we present ‘Substrate Utilisation by Growth and Autotrophic Respiration’ (SUGAR), a simplified model of substrate utilisation, designed to work within an LSM. The aim of the model is to allow the decoupling of PCE and GPP in order to provide a more accurate representation of respiration and growth fluxes, in particular in response to environmental stress. To demonstrate its behaviour and applicability to large scale ecosystem modelling, we use SUGAR to simulate PCE fluxes over the Amazon basin, using GPP data from an ensemble of LSMs, constrained by global fluorescence measurements from the Greenhouse Gases Observing SATellite (GOSAT) (Parazoo et al., 2014) as driving data. We assess the sensitivity of the model to initialised NSC content, within a reasonable range of possible pool sizes and assess the changes the model makes to predictions of ecosystem carbon expenditure. We also test the model under stressed and non-stressed conditions by simulating the world’s longest running tropical rainforest through-fall exclusion (TFE) experiment and corresponding control forest in the Caxiuana National forest, Brazil, over a 16-year period. Previous simulations of the TFE experiment by multiple LSMs has highlighted their inefficiency at capturing the effects of the artificial drought on forest function (Powell et al., 2013). It remains unclear to what extent the lack of NSC dynamics is responsible for the discrepancies between model predictions and observations in these previous studies. We examine the role NSC dynamics has on model predictions during the drought by post processing the output of one of these LSMs, namely the Joint UK Land Environment Simulator (JULES). We compare the results from JULES and the new predictions from SUGAR to observations (Metcalf et al., 2010; da Costa et al., 2014) as well as a time-series of net primary productivity (NPP) derived from data collected in Rowland et al. (2015).

2 Model description

Our ‘Substrate Utilisation by Growth and Autotrophic Respiration (SUGAR)’ model simulates a single pool of carbohydrate at a gridbox scale, for each vegetation tile, and is designed to sit below the photosynthesis component of a LSM (Fig. 1). Assimilated carbon from photosynthesis (GPP) is collected by the NSC pool and the total carbon allocated to respiration and growth is then calculated and taken directly from the NSC pool. The respired carbon is released into the atmosphere and the carbon allocated to growth is given to the demography component of the LSM to be allocated to structural pools. Both growth and respiration depend on temperature and the amount of carbohydrate in the NSC pool relative to the total structural biomass.



4

Simon Jones: A Simple Representation of NSC

2.1 Non-structural carbohydrate pool

The rate of change of NSC content (C_{NSC}) is described by:

$$\frac{dC_{NSC}}{dt} = \Pi_G - R_p - G \quad (1)$$

where Π_G is canopy GPP, R_p is total plant respiration, and G is plant growth.

Using the definition of net primary productivity (Π_N):

$$\Pi_N = \Pi_G - R_p$$

equation (1) is written as:

$$\frac{dC_{NSC}}{dt} = \Pi_N - G \quad (2)$$

To quantify the size of the NSC pool we consider the model under steady state. Under steady state conditions we assume that the NSC mass fraction, defined as the ratio of NSC to structural carbon, is invariant. We denote the steady state mass fraction by f_{NSC} (Eq. (3)), which we also use to initialise the model.

$$f_{NSC} = \left(\frac{C_{NSC}}{C_v} \right)^* \quad (3)$$

where C_v is structural biomass and the asterisk indicates steady state.

2.2 Growth

Plant growth depends on temperature and NSC availability. The temperature dependence is assumed to follow a Q_{10} exponential relationship and the NSC dependence follows Michaelis-Menten reaction kinetics:

$$G = G_0 F_Q(T) C_v \frac{C_{NSC}}{C_{NSC} + K_m C_v} \quad (4)$$

where G_0 (yr^{-1}) is the maximum specific growth rate at the reference temperature 25°C , T ($^\circ\text{C}$) is temperature, C_v (kg C m^{-2}) is total structural carbon biomass, K_m is a half saturation constant equal to the NSC mass fraction at which growth rate is half of its maximum value at the reference temperature and related to the steady state NSC mass fraction by Eq. (6), and $F_Q(T)$ is the Q_{10} temperature dependence given by:

$$F_Q(T) = q_{10}^{0.1(T-25)} = \exp\left(\ln(q_{10}) \frac{(T-25)}{10}\right) \quad (5)$$

where q_{10} , which is a constant taken to be 2.0 by default.

$$K_m = a_{K_m} f_{NSC} \quad (6)$$

and a_{K_m} is a constant with the default value of 0.5

2.3 Respiration

Plant respiration is split into maintenance and growth components. Growth respiration is calculated as a constant fraction of plant growth:

$$R_g = \frac{1 - Y_g}{Y_g} G \quad (7)$$

where Y_g is the growth conversion efficiency, or yield, with a default value of 0.75 (Thornley and Johnson, 1990).

Maintenance respiration has the same temperature and NSC dependence as plant growth:

$$R_m = R_{m_0} F_Q(T) C_v \frac{C_{NSC}}{C_{NSC} + K_m C_v} \quad (8)$$

where R_{m_0} (yr^{-1}) is the maximum specific rate of maintenance respiration at the reference temperature 25°C .



Simon Jones: A Simple Representation of NSC

5

2.4 Total carbohydrate utilisation

The total rate of NSC utilisation, U , is defined as the sum of plant respiration and growth:

$$U = R_p + G \quad (9)$$

U here is exactly equivalent to PCE and is only denoted differently for convenience and ease of reading. Using this definition, Eq. (1) can be written as:

$$\frac{dC_{NSC}}{dt} = \Pi_G - U \quad (10)$$

Since both respiration and growth have the same NSC and temperature dependence, U is given by:

$$U = \phi F_Q(T) C_v \frac{C_{NSC}}{C_{NSC} + K_m C_v} \quad (11)$$

where $\phi = R_{m_0} + \frac{G_0}{Y_g}$ is the maximum specific rate of utilisation of carbohydrate at the reference temperature $25^\circ C$.

2.5 Parameter estimation

10

Values of ϕ , R_{m_0} and G_0 may be found in terms of commonly measurable variables.

First, ϕ is related to the steady state structural carbon turnover time τ , by the parameter a_{K_m} and the steady state Q_{10} function ($F_Q^*(T)$):

$$\phi = \frac{1 + a_{K_m}}{\tau F_Q^*(T)} \quad (12) \quad 15$$

where τ is defined as:

$$\tau = \frac{C_v}{\Pi_G} \quad (13)$$

The parameter α is defined as the ratio of G_0 to ϕ :

$$\alpha = \frac{G_0}{\phi} \quad (14) \quad 20$$

α is set equal to the steady state carbon use efficiency (CUE) of the ecosystem:

$$\alpha = CUE^* \quad (15)$$

G_0 and R_{m_0} are then given by:

$$G_0 = \alpha \frac{1 + a_{K_m}}{\tau F_Q^*(T)} \quad (16)$$

and

$$R_{m_0} = \left(1 - \frac{\alpha}{Y_g}\right) \frac{1 + a_{K_m}}{\tau F_Q^*(T)} \quad (17)$$

Equations (12) and (15) have been derived by considering the model under steady state conditions (see appendix).

Finally, f_{NSC} is set equal to an estimate of ecosystem scale NSC concentration, given as a fraction between 0 and 1. 30



6

Simon Jones: A Simple Representation of NSC

3 Methods

3.1 Sensitivity study over the Amazon-Basin

To demonstrate how SUGAR influences predictions of PCE, we conduct a series of simulations over a six and a half year period from June 2009 to December 2015, across the whole Amazon, where f_{NSC} is varied from 0.0005-0.08. As f_{NSC} represents the initial fraction of the biomass pool that is NSC, a value of 0.0005 is effectively representing a model without NSC. The upper bound of 0.08 is an estimate of the ecosystem NSC content in a tropical forest in Panama (Würth et al., 2005). The model is driven with monthly GPP data from an ensemble of LSMs constrained by global fluorescence measurements from the Greenhouse Gases Observing SATellite (GOSAT) (Parazoo et al., 2014), and temperature data from CRU-JRA (Harris, 2019). An estimate for τ in each grid-box is found using biomass estimates across the Amazon (Avitabile et al., 2016) and the first year of GOSAT GPP. All other parameters (Y_g , a_{K_m} , q_{10}) are kept constant at their default values (see model description).

To assess the effect that the SUGAR model has on the seasonality of PCE, the coefficient of variation of simulated PCE in each grid cell is calculated and presented on a colour-mesh map for each value of f_{NSC} . The Pearson correlation coefficient of simulated PCE and driving GPP, and PCE and the Q_{10} function in each grid cell is also calculated for each value of f_{NSC} and presented on maps.

3.2 Methods - Simulating responses to drought

To evaluate the effectiveness of SUGAR at simulating responses to drought, we tested it at the world's longest tropical drought experiment.

3.2.1 Site Description

The TFE experiment is located in Caxiuanã National Forest, Pará State, Brazil (1°43'3.5"S, 51°27'36"W), where measurements of meteorology and plant physiology of two 1ha plots began in 2001. In January 2002, panels were introduced into one of the plots, excluding c. 50% of rainfall from the soils and subjecting the plot to an artificial drought. Measurements of meteorology and forest physiology continue to the present day (this study looks only up to 2016-12-09). During this period mean annual rainfall was between 1772.6 and 2967.1 mm. Daily incident radiation varied from 419.8 Wm^{-2} to 731.1 Wm^{-2} . A full summary of experimental set up and the most recent collection of results from the site is available in Meir et al. (2018).

At the start of the experiment, total estimated above-ground biomass was 213.9 ± 14.2 $Mgha^{-1}$ in the control forest, and 200.6 ± 13.2 $Mgha^{-1}$ in the TFE plot. After 13 years of the drought treatment, biomass loss to mortality in the TFE plot had increased by $41.0 \pm 2.7\%$ relative to 2001 values (Rowland et al., 2015). Observations and modelling studies at the site suggest that while GPP declined in response to the artificial drought, PCE was maintained at close to pre-drought levels during at least the first 3-4 years of the experiment (Metcalf et al., 2010; Fisher et al., 2007). NSC reserves are thought to have sustained PCE during this time and it is estimated that the forest had access to c. 20 $MgCha^{-1}$ of available NSC (c. 8% of live biomass) during the drought (Metcalf et al., 2010). It is not possible for LSMs to accurately predict both growth and respiration in the TFE forest without simulating some kind of NSC storage, and makes the experiment an ideal opportunity to test SUGAR.

3.2.2 Simulation descriptions

The TFE experiment and corresponding control plot are simulated over the period 2001-01-01 to 2016-12-09. The first set of simulations are conducted using the Joint UK Land Environment Simulator (JULES) (Best et al., 2011; Clark et al., 2011), driven with the meteorological data collected at Caxiuanã. JULES version 5.2 is used with a pre-existing parametrisation of the site and then optimised so that annual GPP and NPP in the control forest agree with observations. The same configuration is then used to simulate the TFE forest. Both control and TFE plot were initialised and spun up for 176 years using a repeated loop of the control meteorological data. To simulate the effect of the drought experiment, precipitation is halved in the TFE simulation from January 1, 2002, in line with estimates of average exclusion rate.

Gridbox GPP (`gpp_gb`) and grid-box temperature at 1.5 m above canopy height (`t1p5m_gb`) outputs from JULES are then used to drive the SUGAR model off-line in each plot. In order to examine how SUGAR compares relative to JULES, it is initialised using the first year of output data from JULES (i.e. the year before panels are put in the TFE plot) rather than



Simon Jones: A Simple Representation of NSC

7

observations from Caxiuanã (with the exception of an estimate of NSC pool size (f_{NSC}), which is necessary given JULES does not model NSC). Since the SUGAR simulations are off-line (i.e. not coupled to a Dynamic Global Vegetation Model (DGVM)) we assume that biomass (C_v) remains constant throughout the experiment. This is a necessary assumption that allows the simulations to be performed off-line and the effect of the NSC pool to be examined in isolation.

3.2.3 Model Evaluation

5

Snapshot fluxes (NPP, R_p , PCE) from JULES and SUGAR are evaluated against observations from (Metcalfe et al., 2010) and (da Costa et al., 2014) for the periods 2005 and 2009-2011. Model growth output is evaluated against an observed time-series of NPP from both plots. Observed NPP is calculated as the sum of observed biomass increment change and total local litterfall (Rowland et al., 2018). Biomass increment is calculated using tree trunk diameter at breast height (DBH) data and a number of allometric equations (Table 2). The DBH data were collected every 1-3 years for each tree in each plot using dendrometers between July 2000 and December 2014. The error bars presented are the sum of measurement error from the litterfall data and the 95% confidence intervals of the ensemble of allometric equations.

10

4 Results

4.1 Sensitivity study over the Amazon-Basin

In simulations of PCE across the Amazon Basin, the SUGAR model dampens the seasonal variations in both respiration and growth, relative to GPP, maintaining a less variable rate of PCE (Fig. 2). The mean coefficient of variation (CV) of the GPP data across the Amazon is 17.6% (bounds: 7.47 – 40.9%, Fig. 2). When the SUGAR model is initialised with $f_{NSC} = 0.0005$, effectively representing a model with no NSC, the mean CV of PCE across the Amazon is 16.5% (bounds: 6.57 – 37.4%, Fig. 2). As f_{NSC} increases the coefficient of variation decreases across all grid boxes. At $f_{NSC} = 0.08$, the mean CV value across the Amazon is 8.96% (bounds: 3.78 – 25.1%, Fig. 2). Increasing the effective size of the NSC pool also reduces the spatial variation in PCE seasonality across Amazonia. Relative to the wetter northern Amazon, the more seasonally dry southern Amazon experiences far greater seasonal variation in GPP. This pattern is mirrored in the seasonal variation of simulated PCE, however, with more NSC in the model the difference between PCE seasonality in the north and south declines, due to a larger decrease in seasonal variation of growth and respiration in the southern regions. This decline in seasonal variation is caused by an increase in dry season carbon expenditure and a decrease in the wet season carbon expenditure. The buffering effect is a consequence of the de-coupling of respiration and growth from GPP, reflected in the decline in the mean correlation coefficient between GPP and PCE from 0.980 (bounds: 0.939 – 1.00) to 0.181 (bounds: -0.501 – 0.997) from simulations with the 0 to 8% mass fraction of NSC (Fig. 3). With this decoupling effect there is also a shift in the primary driver of simulated PCE, from GPP (in the 0% NSC mass fraction simulation) to the Q_{10} function (in the 8% NSC mass fraction simulation). This is reflected in the increase in the mean correlation coefficient between simulated PCE and the Q_{10} function (Eq. (5)) in SUGAR from -0.0485 (bounds: -0.651 to 0.517) to 0.637 (bounds: -0.456 to 0.956) in the 0 to 8% NSC mass fraction simulations (Fig. 4).

15

20

25

30

4.2 Simulations in a tropical moist forest

In the simulations of the control plot, in which the forest was not subject to any artificial drought stress, JULES and SUGAR produce similar results of long term NPP accumulation (Fig. 5), that are both consistent with observations. By the end of the NPP observation period (2014-12-17), JULES predicts a total accumulated NPP of 155.6 MgCha⁻¹ and SUGAR 154.7 MgCha⁻¹. Both results are consistent with observations (Fig. 5, 161.5±22.0 MgCha⁻¹) from the site.

35

There are some larger differences between JULES and SUGAR on annual time-scales, but in general the models predict comparable annual mean values of control plot PCE, R_a and NPP (Fig. 6). During the first three years of the experiment (2002, 2003, 2004), JULES predicts an annual mean PCE of 35.13 MgCha⁻¹yr⁻¹, and SUGAR predicts 34.79 MgCha⁻¹yr⁻¹. Both these results lie within the confidence intervals of the observations from the site (Fig. 6, 33.0±2.9 MgCha⁻¹yr⁻¹). The two models differ most in the natural drought years of 2005, 2010 and 2015 in which predicted annual GPP is at its lowest. In 2005 JULES predicts a decrease (relative to the 2002-2004 period) in annual mean PCE to 33.32 MgCha⁻¹yr⁻¹ (-5.15%) whereas SUGAR predicts an increase to 36.18 MgCha⁻¹yr⁻¹ (+4.00%). The decrease in JULES PCE is caused by a decrease in predicted GPP in 2005. In SUGAR this decrease in GPP is buffered by NSC storage, and increase in the annual mean temperature drives the increase in predicted PCE. Both results are close to the observed value although the SUGAR result is outside the observed confidence intervals by 0.780%. In 2010 average annual rainfall was 1772.6 mm yr⁻¹, the lowest in the

40

45



16 year period (c. 25% decrease on the 16-year mean 2324.2 mmyr^{-1}). This causes a decline in predicted GPP on the control plot from $35.92 \text{ MgCha}^{-1}\text{yr}^{-1}$ in 2008 to $32.94 \text{ MgCha}^{-1}\text{yr}^{-1}$ in 2010. Consequently, JULES predicts a mean PCE of $33.60 \text{ MgCha}^{-1}\text{yr}^{-1}$ over the period 2009-2011 which lies below observed values. SUGAR is able to buffer the forest against the 2010 decline in GPP and allows elevated PCE in 2010 ($36.52 \text{ MgCha}^{-1}\text{yr}^{-1}$) relative to 2008 ($34.53 \text{ MgCha}^{-1}\text{yr}^{-1}$).
5 This allows SUGAR to maintain a mean PCE value over the 2009-2011 period of $36.07 \text{ MgCha}^{-1}\text{yr}^{-1}$ which is close to observations (Fig. 6).

4.3 Simulating responses to drought

In the TFE plot simulations, SUGAR and JULES diverge significantly in their predictions of NPP, PCE and Ra, with SUGAR more accurately capturing observations than JULES (Figs. 5&6). JULES is able to capture NPP accumulation for approximately 1 year after the start of the drought treatment, however, from 2003 onwards, predicted NPP accumulation drops significantly below the confidence intervals of the observations (Fig. 5). This is driven predominantly by a sharp decline in GPP in response to the declining water availability. SUGAR is able to capture NPP accumulation for much longer and predictions remain within the confidence intervals of the observations until the start of 2009 (Fig. 5). By the end of the observation period JULES predicts a total of 60.6 MgCha^{-1} of accumulated and SUGAR 105.8 MgCha^{-1} . Neither result lies within observed confidence intervals of the observations (Fig. 5, $126.8 \pm 16.9 \text{ MgCha}^{-1}$) although the SUGAR result represents a significant improvement relative to JULES.
10
15

During the first 3 years of the experiment, SUGAR is able to buffer a significant decline in predicted GPP on the TFE plot, which drops from $34.90 \text{ MgCha}^{-1}\text{yr}^{-1}$ in 2001, to a minimum of $19.61 \text{ MgCha}^{-1}\text{yr}^{-1}$ in 2003 (-43.8%). Since JULES does not contain an NSC storage component and PCE is equal to GPP, PCE in JULES also drops by 43.8%, from $34.90 \text{ MgCha}^{-1}\text{yr}^{-1}$ in 2001 to $19.61 \text{ MgCha}^{-1}\text{yr}^{-1}$ in 2003. As a result JULES predicts a mean PCE value of $24.84 \text{ MgCha}^{-1}\text{yr}^{-1}$ over the first three years of drought treatment (2002,2003,2004). These values are outside the confidence intervals of the observations and 26.7% below the mean PCE value observed in the TFE plot ($33.9 \pm 3.6 \text{ MgCha}^{-1}\text{yr}^{-1}$, Fig. 6). The SUGAR model is able to maintain PCE at a higher level than JULES during these first three years by drawing upon a mean 5.53 MgCha^{-1} of NSC each year to support growth and respiration. This results in a mean PCE of $30.37 \text{ MgCha}^{-1}\text{yr}^{-1}$ over the period 2002-2004, which lies within the observed confidence interval (Fig. 6). The NSC buffering effect in SUGAR continues in 2005 with SUGAR expending 5.80 MgCha^{-1} more carbon than JULES during that year. This means that the predicted annual mean PCE in SUGAR is $23.03 \text{ MgCha}^{-1}\text{yr}^{-1}$ compared to $17.23 \text{ MgCha}^{-1}\text{yr}^{-1}$ in JULES. Both results lie below the lower bound of the observed confidence intervals ($33.9 \pm 3.6 \text{ MgCha}^{-1}\text{yr}^{-1}$, Fig. 6), however, the SUGAR result represents a significant improvement relative to JULES. In the latter years of the drought simulations (2009 onwards), the NSC pool becomes significantly depleted and the buffering effect in SUGAR (described above) diminishes. Consequently, on annual time-scales, the mean PCE in JULES and SUGAR during the 2009-2011 period are similar (20.76 and $21.21 \text{ MgCha}^{-1}\text{yr}^{-1}$ respectively), although the allocation of carbon to respiration and growth is different, with SUGAR expending more ($6.70 \text{ MgCha}^{-1}\text{yr}^{-1}$) carbon on growth than JULES ($3.06 \text{ MgCha}^{-1}\text{yr}^{-1}$). This difference in allocation allows SUGAR to predict the observed NPP with more skill than JULES, however it means that respiration predictions are reduced relative to JULES and the observations.
20
25
30
35

5 Discussion

SUGAR alters the relationship between photosynthesis and carbon expenditure. This has implications for simulations of both extreme and more gradual changes in climatic and meteorological conditions. By decoupling PCE from GPP, SUGAR creates a buffering effect that decreases the seasonal variation of carbon expenditure, even in ecosystems where the variation of GPP is already low. As we increase the levels of stored substrate within our simulations, the variability in PCE declines, due to an increased ability to maintain respiration and growth when GPP is low, and replenishment of the NSC pool when GPP is high. This effect is most pronounced in the semi-arid regions of the southern Amazon where there is a strong seasonal cycle in GPP (Fig. A1), corresponding to a strong seasonal pattern of precipitation. Semi-arid regions provide the largest contribution to the global carbon sink anomaly, in part due to this high variability in GPP (Poulter et al., 2014; Ahlström et al., 2015). To represent this contribution, land surface models must capture the response of vegetation to the climate variability experienced in these regions now and in the future. SUGAR provides a mechanistic approach to achieve this by simulating respiration and NPP as a separate function to GPP. Given the strong evidence from observations that NPP and respiration do not have the same seasonal and climatic responses as GPP (Liu et al., 2017; Girardin et al., 2016; Doughty et al., 2015a), accurately predicting future variability in atmospheric CO_2 concentrations (Cox et al., 2013) will be reliant on a sub-model such as
40
45
50



Simon Jones: A Simple Representation of NSC

9

SUGAR which can allow this de-coupling to occur. Research demonstrating the importance of highly seasonal arid regions highlights the necessity of substrate-based approaches in large scale ecosystem models and should motivate the community to focus on improving our understanding of NSCs and how to model them.

The sensitivity of the biosphere to climate change has large impacts on the future climate. For example, large losses of tropical forest carbon may represent a tipping point in the climate system that could have highly adverse and irreversible consequences for the global climate (Cox et al., 2000). However, both the nature and likelihood of such a tipping point is uncertain. Feedbacks between the climate and the carbon cycle mean that small perturbations in the state of the biosphere can make significant changes to the future state of the climate (Friedlingstein et al., 2001). Small changes in the sensitivity of a tropical forest to climate change, may be the difference between the continued absorption of CO₂ by ecosystems such as the Amazon, and the severe die-back scenarios predicted by some models (Huntingford et al., 2013; Phillips et al., 2009). Therefore the difference between a forest that is able to buffer the effects of even a short drought or reduction in productivity, and a forest that is not, may be significant at a global context in the future, even if it appears small in the present day. Non-conservative propagation of perturbations in the state of vegetated ecosystems contributes to large uncertainty in climate models (Huntingford et al., 2009), which greatly reduces our ability to constrain future climate possibilities and tipping points within the carbon-cycle. Accurately representing the response of forest biomass, particularly in the tropics, to changes in climate is crucial to reducing this uncertainty and is a major goal of the climate and land surface modelling community. The buffering effect demonstrated in SUGAR may have an indirect yet large impact on the predictions of future climate by LSMs and provide a more realistic representation of forest sensitivity to climate.

As well as a buffering of carbon expenditure, SUGAR also enables a transition of the primary driver of growth and respiration. With little or no carbohydrate, carbon expenditure in SUGAR is driven predominantly by the rate of photosynthesis (Fig 4). Carbon is used by the ecosystem as soon as it is assimilated, meaning that the rate of expenditure is highly correlated with the rate of photosynthesis. This is often described as ‘source driven carbon dynamics’ meaning that photosynthesis is the key driving flux in determining the carbon balance of the ecosystem. ‘Source driven carbon dynamics’ are at the centre of many LSMs including JULES. As more carbohydrate is added to the ecosystem in SUGAR, temperature becomes the predominant driver of PCE via the Q₁₀ function (Eq. (5), Fig. 4). As more carbon is stored, growth and respiration become less carbon limited and more controlled by the Q₁₀ function within SUGAR. This shift can be seen as a transition towards ‘sink driven carbon dynamics’. Under the theory of sink driven carbon dynamics, environmental variables such as temperature and water-availability exert a direct control over carbon expenditure that can be larger than that of photosynthesis (Körner, 2003; Wiley and Helliker, 2012; Palacio et al., 2014; Fatichi et al., 2014). Processes such as end-product inhibition (Stitt, 1991), in which photosynthesis is inhibited by an excess of assimilate in the leaves, mean that growth and respiration may even exert indirect control over the rate of photosynthesis. The result is that ‘sink’ fluxes (i.e respiration and growth), driven by environmental variables, are the predominant determinants of ecosystem carbon balance. Since the NSC pool in SUGAR does not exert any control over photosynthesis (e.g. via end-product inhibition) the behaviour of SUGAR here cannot be described as truly sink driven. However, SUGAR provides a framework that allows processes such as end-product inhibition to be implemented, and so provides the opportunity to represent both sink and source driven dynamics in LSMs. This allows a greater representation of how the limiting factors of growth and respiration interact with, and respond to a changing climate.

Using the Caxiuanã control simulations we demonstrate that SUGAR and JULES predict very similar long-term NPP accumulation in the natural climate conditions of a tropical moist forest. However, there are larger differences between SUGAR and JULES on an annual time-scale, due to the buffering of the natural variability in GPP by SUGAR. These results further highlight the importance of substrate-based modelling to better capture the responses to natural variation, even under current climate conditions and without extreme events (Doughty et al., 2015a). In the TFE plot, SUGAR makes significant improvements to the prediction of ecosystem carbon fluxes, particularly for accumulated NPP. This improvement is caused by a combination of two processes that occur in SUGAR and that are not present in JULES. The first process is the utilisation of the NSC pool during the early stages of the experiment. SUGAR expends a mean 5.53 Mgha⁻¹ more carbon than is assimilated through photosynthesis in the first three years of drought (2002-2004) and a further 5.80 Mgha⁻¹ in 2005. This allows an increase in both NPP and respiration relative to JULES and is consistent with the analysis in Metcalfe et al. (2010), which suggests the TFE plot was expending 7±4.5 MgCha⁻¹yr⁻¹ more than it was accumulating in 2005, implying that NSC stores were being depleted in response to the drought. The second process is the down regulation of respiration in response to the depleting NSC pool. In the JULES simulations, photosynthesis declines much faster than respiration and, since growth is equal to GPP – Ra in JULES, this means that NPP drops significantly as GPP declines in response to the drought. The result of this effect is that in two years (2005 and 2007), the predicted annual mean NPP by JULES, is negative. Negative NPP is generally considered to be unrealistic, particularly over the time-scale of a year (Roxburgh et al., 2005), and since JULES



does not contain a labile carbon pool to support the deficit, missing carbon is taken from the structural pool. The physical interpretation of this is that trees in JULES respire away their structural carbon and shrink. While there is some evidence of recycling and remobilisation of structural compounds, the magnitude of structural carbon being allocated to respiration (via the resulting negative NPP) in these JULES simulations is not realistic. In SUGAR, respiration declines due to the depletion of the NSC pool. This down-regulation of R_a means that a larger proportion of instantaneous GPP is available for NPP, resulting in larger predictions of NPP in SUGAR than JULES, despite similar estimates of total PCE. While NPP ($GPP - R_a$) may be negative in SUGAR when respiration exceeds photosynthesis, the growth flux that is sent to the structural pools (Eq. (4)) has a lower bound of zero. This eliminates the possibility of unrealistic negative growth rates and the respiration of structural carbon.

The ability of SUGAR to accurately capture PCE responses to drought is somewhat limited by the GPP used to run it. Photosynthesis in JULES has a high sensitivity to reductions in soil moisture (eg., Harper et al., 2016; Williams et al., 2018). In the Caxiuana simulations JULES predicts an average decline in annual GPP of $4.42 \text{ MgCha}^{-1}\text{yr}^{-1}$ from 2001 to 2005 in the TFE plot. Combining the observed PCE rates in the TFE plot with the predicted GPP by JULES would imply that the forest is using an average of $10.96 \text{ MgCha}^{-1}\text{yr}^{-1}$ carbon more than it is assimilating in the first four years. This would then imply that the forest has access to at least 43.86 MgC/ha of NSC, c. 22% of estimated forest biomass. Such a high NSC content is unlikely for tropical forests, which are more likely to have reserves close to 10% (Würth et al., 2005). The other, and more likely explanation is that JULES is overestimating the decline in photosynthesis in response to the drought. The recent work to improve stomatal responses to drought stress (Mencuccini et al., 2019; Eller et al., 2018; Sperry et al., 2017) has the potential to significantly improve GPP predictions in LSMs such as JULES. However, there is a clear link between hydraulics and labile carbon storage, given stomatal closure comes at the cost of a reduction in carbon assimilation. The ability of a plant to store and use labile carbon is crucial to its ability to survive, and recover from, drought-induced stomatal closure (Sala and Mencuccini, 2014; O'Brien et al., 2014; Trugman et al., 2018). Without including at least simple representations of NSC storage, the potential of this recent work to improve the representation of stomatal behaviour in response to drought in LSMs, is unlikely to be realised.

SUGAR is a purposefully simple model of NSC storage and is missing some key processes known to be important in defining the complexities of NSC storage and use within a plant. A more complex NSC model might, for example, distinguish between starch and sugar pools, or represent multiple pools for each plant organ, and actively control the input or output of NSC into pools (Martínez-Vilalta et al., 2016; Hartmann and Trumbore, 2016). However, such models would likely require representation of substrate transport between pools and the scaling of NSC values to the level of trees and forests. Recent advancements in measurement protocols may allow these datasets to be reliably collected (Landhäusser et al., 2018), however, previously the level of uncertainty on such figures has been up to 400% (Quentin et al., 2015). As a result, comprehensive NSC data-sets, measured through time in response to climatic variations and across enough biomes to allow all model PFTs to be evaluated are currently not available. Therefore, this is not a currently viable way to constrain model output. Instead SUGAR is designed to break the direct link between PCE and GPP found in many LSMs and to provide more mechanistic predictions of growth and respiration. It can be parametrised, initialised and evaluated with data that is commonly collected across the globe – Biomass, GPP and temperature (to calculate carbon residency time); CUE (to find α); and respiration and NPP (for evaluation). It also requires an input of initialised NSC fraction (f_{NSC}) which is not easily measured for an ecosystem, although values of f_{NSC} can be constrained within sensible bounds (Würth et al., 2005). It may also be possible to use SUGAR as a tool to further constrain observed values of NSC content by conducting sensitivity studies of f_{NSC} . Given the existing level of knowledge, it is more robust and realistic to use a simple model such as SUGAR which can be evaluated against more easily available observations such as R_a , PCE, NPP and GPP. As the accuracy and spatial extent of NSC data grows models such as SUGAR can act as a simple skeleton that allows new processes to be implemented into LSMs, to more accurately represent the complexity of plant carbon storage and use.

6 Conclusions

We have developed a simple model of NSC storage, designed to be integrated into an LSM. The model makes significant changes to the variability of growth and respiration predictions in both extreme and more stable climatic conditions. This has large implications for simulations of future climate given the importance of predicting the variability of atmospheric CO_2 concentrations. The model also allows a more mechanistic representation of the limiting factors of carbon expenditure which may become increasingly important as the climate changes in the future. Due to the simplicity of the model it is easily parametrised using pre-existing data and does not require complex datasets of NSC storage which are currently unavailable. This makes



Simon Jones: A Simple Representation of NSC

11

the model attractive since it can be easily integrated into LSMs without introducing unreasonable uncertainty in parameter values. The magnitude of the change demonstrates the importance of representing carbon storage in LSMs and we hope will motivate both the modelling and empirical communities to further develop our understanding and model representation of NSC dynamics.

Code availability. A model example of SUGAR for a single site and set up to run at Caxiuaná using output from JULES is available at <http://doi.org/10.5281/zenodo.3547613> For further information or code please contact sj326@exeter.ac.uk

Appendix A: Derivation of model parameters

A1 Derivation of ϕ

The NSC model is parametrised using steady state data where the NSC pool can be assumed to be in equilibrium. Equation (10) is integrated over the data period, P .

$$\frac{1}{P} \int_t^{t+P} \frac{dC_{NSC}}{dt} dt = \frac{1}{P} \int_t^{t+P} \Pi_G - U dt \quad (\text{A1})$$

Using the assumption that the non-structural carbohydrate pools are approximately invariant over this period, it follows that:

$$\frac{dC_{NSC}^*}{dt} \approx 0 \quad (\text{A2})$$

and

$$U^* \approx \phi F_Q^*(T) C_v^* \frac{C_{NSC}^*}{C_{NSC}^* + K_m C_v^*} \quad (\text{A3})$$

where the asterisk denotes temporal averaging. i.e for variable $X(t)$:

$$X^* = \frac{1}{P} \int_t^{t+P} X(t) dt$$

Substituting Eq. (A2) and Eq. (A3) into Eq. (A1) and rearranging using Eq. (3), results in the expression:

$$\phi = \frac{\Pi_G^*}{C_{NSC}^* F_Q^*} (f_{NSC} + K_m) \quad (\text{A4})$$

Using Eq. (6), this is further simplified to:

$$\phi = \frac{\Pi_G^*}{C_{NSC}^* F_Q^*} (1 + a_{K_m}) f_{NSC} \quad (\text{A5})$$

and using Eq. (3), this becomes:

$$\phi = \frac{\Pi_G^*}{C_v^* F_Q^*} (1 + a_{K_m}) \quad (\text{A6})$$

Using

$$\tau = \frac{C_v}{\Pi_G} \quad (\text{A7})$$

where τ is the turnover time of structural carbon of the ecosystem, which under steady state conditions is equal to structural carbon residency time, ϕ is given by:

$$\phi = \frac{1 + a_{K_m}}{\tau F_Q^*(T)} \quad (\text{A8})$$



A2 Derivation of α

Using Eq. (4) & Eq. (11), the ratio of growth to PCE is:

$$\frac{G}{U} = \frac{G_0}{\phi} \quad (\text{A9})$$

which is, by definition, equal to α . Under steady state conditions growth is equal to NPP and PCE is equal to GPP (from Eq. (2) and Eq. (10)). Hence it follows that:

$$\alpha = \frac{\Pi_N^*}{\Pi_G^*} \quad (\text{A10})$$

i.e. α is equal to the steady state, or mean carbon use efficiency of the ecosystem during the parametrisation period.

Author contributions. SJ, LR, PC, DH and AH developed the SUGAR model code and SJ carried out the simulations. JULES simulations were conducted by SJ with contributions from AH and KW. GPP data from GOSAT were provided by NP. Data from the through-fall exclusion experiment in Caxiuana were provided by AdC, PM and LR. SJ prepared the manuscript with contributions from all co-authors.

Competing interests. The authors declare that they have no conflict of interest

Acknowledgements. This work has been funded by the Natural Environmental Research Council NE/L002434/1. LR was supported by the UK NERC independent fellowship grant NE/N014022/1. KW was supported by the Newton Fund through the Met Office Climate Science for Service Partnership Brazil (CSSP Brazil). PM was supported by NERC NE/N006852/1 and ARC DP170104091. MM was supported by the Spanish Ministry of Economy and Competitiveness (MINECO) via competitive grants CGL2013-46808-R and CGL2017-89149-C2-1-R. AH acknowledges funding from EPSRC Fellowship EP/N030141/1.

References

- Adams, H. D., Germino, M. J., Breshears, D. D., Barron-Gafford, G. A., Guardiola-Claramonte, M., Zou, C. B., and Huxman, T. E.: Non-structural leaf carbohydrate dynamics of *Pinus edulis* during drought-induced tree mortality reveal role for carbon metabolism in mortality mechanism, *New Phytologist*, 197, 1142–1151, <https://doi.org/10.1111/nph.12102>, <https://nph.onlinelibrary.wiley.com/doi/abs/10.1111/nph.12102>, 2013.
- Adams, H. D., Zeppel, M. J. B., Anderegg, W. R. L., Hartmann, H., Landhäusser, S. M., Tissue, D. T., Huxman, T. E., Hudson, P. J., Franz, T. E., Allen, C. D., Anderegg, L. D. L., Barron-Gafford, G. A., Beerling, D. J., Breshears, D. D., Brodrribb, T. J., Bugmann, H., Cobb, R. C., Collins, A. D., Dickman, L. T., Duan, H., Ewers, B. E., Galiano, L., Galvez, D. A., Garcia-Forner, N., Gaylord, M. L., Germino, M. J., Gessler, A., Hacke, U. G., Hakamada, R., Hector, A., Jenkins, M. W., Kane, J. M., Kolb, T. E., Law, D. J., Lewis, J. D., Limousin, J.-M., Love, D. M., Macalady, A. K., Martínez-Vilalta, J., Mencuccini, M., Mitchell, P. J., Muss, J. D., O'Brien, M. J., O'Grady, A. P., Pangle, R. E., Pinkard, E. A., Piper, F. I., Plaut, J. A., Pockman, W. T., Quirk, J., Reinhardt, K., Ripullone, F., Ryan, M. G., Sala, A., Sevanto, S., Sperry, J. S., Vargas, R., Vennetier, M., Way, D. A., Xu, C., Yezpez, E. A., and McDowell, N. G.: A multi-species synthesis of physiological mechanisms in drought-induced tree mortality, *Nature Ecology & Evolution*, 1, 1285–1291, <https://doi.org/10.1038/s41559-017-0248-x>, 2017.
- Ahlström, A., Raupach, M. R., Schurgers, G., Smith, B., Arneeth, A., Jung, M., Reichstein, M., Canadell, J. G., Friedlingstein, P., Jain, A. K., Kato, E., Poulter, B., Sitch, S., Stocker, B. D., Viovy, N., Wang, Y. P., Wiltshire, A., Zaehle, S., and Zeng, N.: The dominant role of semi-arid ecosystems in the trend and variability of the land CO₂ sink, *Science*, 348, 895–899, <https://doi.org/10.1126/science.aaa1668>, <https://science.sciencemag.org/content/348/6237/895>, 2015.
- Anderegg, W. R. and Anderegg, L. D.: Hydraulic and carbohydrate changes in experimental drought-induced mortality of saplings in two conifer species, *Tree Physiology*, 33, 252–260, <https://doi.org/10.1093/treephys/tpu016>, <https://doi.org/10.1093/treephys/tpu016>, 2013.
- Arora, V. K., Boer, G. J., Friedlingstein, P., Eby, M., Jones, C. D., Christian, J. R., Bonan, G., Bopp, L., Brovkin, V., Cadule, P., Hajima, T., Ilyina, T., Lindsay, K., Tjiputra, J. F., and Wu, T.: Carbon–Concentration and Carbon–Climate Feedbacks in CMIP5 Earth System Models, *Journal of Climate*, 26, 5289–5314, <https://doi.org/10.1175/JCLI-D-12-00494.1>, <https://doi.org/10.1175/JCLI-D-12-00494.1>, 2013.
- Avitabile, V., Herold, M., Heuvelink, G. B. M., Lewis, S. L., Phillips, O. L., Asner, G. P., Armston, J., Ashton, P. S., Banin, L., Bayol, N., Berry, N. J., Boeckx, P., de Jong, B. H. J., DeVries, B., Girardin, C. A. J., Kearsley, E., Lindsell, J. A., Lopez-Gonzalez, G., Lucas, R., Malhi, Y., Morel, A., Mitchard, E. T. A., Nagy, L., Qie, L., Quinones, M. J., Ryan, C. M., Ferry, S. J. W., Sunderland, T., Laurin, G. V., Gatti, R. C., Valentini, R., Verbeeck, H., Wijaya, A., and Willcock, S.: An integrated pan-tropical biomass map using multiple reference datasets, *Global Change Biology*, 22, 1406–1420, <https://doi.org/10.1111/gcb.13139>, <https://onlinelibrary.wiley.com/doi/abs/10.1111/gcb.13139>, 2016.



Simon Jones: A Simple Representation of NSC

13

- Baker, I. T., Prihodko, L., Denning, A. S., Goulden, M., Miller, S., and da Rocha, H. R.: Seasonal drought stress in the Amazon: Reconciling models and observations, *Journal of Geophysical Research: Biogeosciences*, 113, <https://doi.org/10.1029/2007JG000644>, <https://agupubs.onlinelibrary.wiley.com/doi/abs/10.1029/2007JG000644>, 2008.
- Bastos, A., Friedlingstein, P., Sitch, S., Chen, C., Mialon, A., Wigneron, J.-P., Arora, V. K., Briggs, P. R., Canadell, J. G., Ciais, P., Chevallier, F., Cheng, L., Delire, C., Haverd, V., Jain, A. K., Joos, F., Kato, E., Lienert, S., Lombardozzi, D., Melton, J. R., Myneni, R., Nabel, J. E. M. S., Pongratz, J., Poulter, B., Rödenbeck, C., Séférian, R., Tian, H., van Eck, C., Viovy, N., Vuichard, N., Walker, A. P., Wiltshire, A., Yang, J., Zaehle, S., Zeng, N., and Zhu, D.: Impact of the 2015/2016 El Niño on the terrestrial carbon cycle constrained by bottom-up and top-down approaches, *Philosophical Transactions of the Royal Society B: Biological Sciences*, 373, 20170304, <https://doi.org/10.1098/rstb.2017.0304>, <https://royalsocietypublishing.org/doi/abs/10.1098/rstb.2017.0304>, 2018.
- Best, M. J., Pryor, M., Clark, D. B., Rooney, G. G., Essery, R. L. H., Ménard, C. B., Edwards, J. M., Hendry, M. A., Porson, A., Gedney, N., Mercado, L. M., Sitch, S., Blyth, E., Boucher, O., Cox, P. M., Grimmond, C. S. B., and Harding, R. J.: The Joint UK Land Environment Simulator (JULES), model description - Part 1: Energy and water fluxes, *Geoscientific Model Development*, 4, 677–699, <https://doi.org/10.5194/gmd-4-677-2011>, <https://www.geosci-model-dev.net/4/677/2011/>, 2011.
- Clark, D. B., Mercado, L. M., Sitch, S., Jones, C. D., Gedney, N., Best, M. J., Pryor, M., Rooney, G. G., Essery, R. L. H., Blyth, E., Boucher, O., Harding, R. J., Huntingford, C., and Cox, P. M.: The Joint UK Land Environment Simulator (JULES), model description - Part 2: Carbon fluxes and vegetation dynamics, *Geoscientific Model Development*, 4, 701–722, <https://doi.org/10.5194/gmd-4-701-2011>, <https://www.geosci-model-dev.net/4/701/2011/>, 2011.
- Corlett, R. T.: The Impacts of Droughts in Tropical Forests, *Trends in Plant Science*, 21, 584 – 593, <https://doi.org/https://doi.org/10.1016/j.tplants.2016.02.003>, <http://www.sciencedirect.com/science/article/pii/S1360138516000571>, 2016.
- Cox, P., Betts, R. A., Jones, C., Spall, S. A., and Totterdell, I. J.: Acceleration of global warming due to carbon-cycle feedbacks in a coupled model, *Nature*, 408, 2000.
- Cox, P. M., Pearson, D., Booth, B. B., Friedlingstein, P., Huntingford, C., Jones, C. D., and Luke, C. M.: Sensitivity of tropical carbon to climate change constrained by carbon dioxide variability, *Nature*, 494, <https://doi.org/10.1038/nature11882>, <https://doi.org/10.1038/nature11882>, 2013.
- da Costa, A. C. L., Galbraith, D., Almeida, S., Portela, B. T. T., da Costa, M., de Athaydes Silva Junior, J., Braga, A. P., de Gonçalves, P. H. L., de Oliveira, A. A., Fisher, R., Phillips, O. L., Metcalfe, D. B., Levy, P., and Meir, P.: Effect of 7 yr of experimental drought on vegetation dynamics and biomass storage of an eastern Amazonian rainforest, *New Phytologist*, 187, 579–591, <https://doi.org/10.1111/j.1469-8137.2010.03309.x>, <https://nph.onlinelibrary.wiley.com/doi/abs/10.1111/j.1469-8137.2010.03309.x>, 2010.
- da Costa, A. C. L., Metcalfe, D. B., Doughty, C. E., de Oliveira, A. A., Neto, G. F., da Costa, M. C., Silva Junior, J. d. A., Aragão, L. E., Almeida, S., Galbraith, D. R., Rowland, L. M., Meir, P., and Malhi, Y.: Ecosystem respiration and net primary productivity after 8–10 years of experimental through-fall reduction in an eastern Amazon forest, *Plant Ecology & Diversity*, 7, 7–24, <https://doi.org/10.1080/17550874.2013.798366>, <https://doi.org/10.1080/17550874.2013.798366>, 2014.
- De Kauwe, M. G., Medlyn Belinda, E., Zaehle, S., Walker, A. P., Dietze, M. C., Wang, Y., Luo, Y., Jain, A. K., El-Masri, B., Hickler, T., Wårlind, D., Weng, E., Parton, W. J., Thornton, P. E., Wang, S., Prentice, I. C., Asao, S., Smith, B., McCarthy, H. R., Iversen, C. M., Hanson, P. J., Warren, J. M., Oren, R., and Norby, R. J.: Where does the carbon go? A model–data intercomparison of vegetation carbon allocation and turnover processes at two temperate forest free-air CO₂ enrichment sites, *New Phytologist*, 203, 883–899, <https://doi.org/10.1111/nph.12847>, <https://nph.onlinelibrary.wiley.com/doi/abs/10.1111/nph.12847>, 2014.
- Dewar, R. C., Medlyn, B. E., and Mcmurtrie, R. E.: Acclimation of the respiration/photosynthesis ratio to temperature: insights from a model, *Global Change Biology*, 5, 615–622, <https://doi.org/10.1046/j.1365-2486.1999.00253.x>, <https://onlinelibrary.wiley.com/doi/abs/10.1046/j.1365-2486.1999.00253.x>, 1999.
- Dietze, M. C., Sala, A., Carbone, M. S., Czimeczik, C. I., Mantooth, J. A., Richardson, A. D., and Vargas, R.: Nonstructural Carbon in Woody Plants, *Annual Review of Plant Biology*, 65, 667–687, <https://doi.org/10.1146/annurev-arplant-050213-040054>, <https://doi.org/10.1146/annurev-arplant-050213-040054>, PMID: 24274032, 2014.
- Doughty, C. E., Metcalfe, D. B., Girardin, C. A. J., Amézquita, F. F., Durand, L., Huaraca Huasco, W., Silva-Espejo, J. E., Araujo-Murakami, A., da Costa, M. C., da Costa, A. C. L., Rocha, W., Meir, P., Galbraith, D., and Malhi, Y.: Source and sink carbon dynamics and carbon allocation in the Amazon basin, *Global Biogeochemical Cycles*, 29, 645–655, <https://doi.org/10.1002/2014GB005028>, <https://agupubs.onlinelibrary.wiley.com/doi/abs/10.1002/2014GB005028>, 2015a.
- Doughty, C. E., Metcalfe, D. B., Girardin, C. A. J., Amézquita, F. F., Cabrera, D. G., Huasco, W. H., Silva-Espejo, J. E., Araujo-Murakami, A., da Costa, M. C., Rocha, W., Feldpausch, T. R., Mendoza, A. L. M., da Costa, A. C. L., Meir, P., Phillips, O. L., and Malhi, Y.: Drought impact on forest carbon dynamics and fluxes in Amazonia, *Nature*, 519, 78–82, <https://doi.org/10.1038/nature14213>, <https://doi.org/10.1038/nature14213>, 2015b.
- Eller, C. B., Rowland, L., Oliveira, R. S., Bittencourt, P. R. L., Barros, F. V., da Costa, A. C. L., Meir, P., Friend, A. D., Mencuccini, M., Sitch, S., and Cox, P.: Modelling tropical forest responses to drought and El Niño with a stomatal optimization model based on xylem hydraulics, *Philosophical Transactions of the Royal Society B: Biological Sciences*, 373, 20170315, <https://doi.org/10.1098/rstb.2017.0315>, <https://royalsocietypublishing.org/doi/abs/10.1098/rstb.2017.0315>, 2018.
- Faticchi, S., Leuzinger, S., and Körner, C.: Moving beyond photosynthesis: from carbon source to sink-driven vegetation modeling, *New Phytologist*, 201, 1086–1095, <https://doi.org/10.1111/nph.12614>, <http://dx.doi.org/10.1111/nph.12614>, 2014.



- Fatichi, S., Pappas, C., and Ivanov, V. Y.: Modeling plant–water interactions: an ecohydrological overview from the cell to the global scale, *Wiley Interdisciplinary Reviews: Water*, 3, 327–368, <https://doi.org/10.1002/wat2.1125>, <https://onlinelibrary.wiley.com/doi/abs/10.1002/wat2.1125>, 2016.
- Fatichi, S., Pappas, C., Zscheischler, J., and Leuzinger, S.: Modelling carbon sources and sinks in terrestrial vegetation, *New Phytologist*, 221, 652–668, <https://doi.org/10.1111/nph.15451>, <https://nph.onlinelibrary.wiley.com/doi/abs/10.1111/nph.15451>, 2019.
- Fisher, R. A., Williams, M., Da Costa, A. L., Malhi, Y., Da Costa, R. F., Almeida, S., and Meir, P.: The response of an Eastern Amazonian rain forest to drought stress: results and modelling analyses from a throughfall exclusion experiment, *Global Change Biology*, 13, 2361–2378, <https://doi.org/10.1111/j.1365-2486.2007.01417.x>, <https://onlinelibrary.wiley.com/doi/abs/10.1111/j.1365-2486.2007.01417.x>, 2007.
- Friedlingstein, P., Bopp, L., Philippe, C., Jean-Louis, D., Laurent, F., Hervé, L., Patrick, M., and James, O.: Positive feedback between future climate change and the carbon cycle, *Geophysical Research Letters*, 28, 1543–1546, <https://doi.org/10.1029/2000GL012015>, <https://agupubs.onlinelibrary.wiley.com/doi/abs/10.1029/2000GL012015>, 2001.
- Fritts, H. C., Shashkin, A. V., Hemming, D. L., Leavitt, S. W., Wright, W. E., and Downs, G. M.: Preliminary Draft User Manual for Treering 2000, <https://www.ltrr.arizona.edu/~hal/treering/manual2000.PDF>, 2000.
- Galiano, L., Martínez-Vilalta, J., and Lloret, F.: Carbon reserves and canopy defoliation determine the recovery of Scots pine 4 yr after a drought episode, *New Phytologist*, 190, 750–759, <https://doi.org/10.1111/j.1469-8137.2010.03628.x>, <https://nph.onlinelibrary.wiley.com/doi/abs/10.1111/j.1469-8137.2010.03628.x>, 2011.
- Gatti, L. V., Gloor, M., Miller, J. B., Doughty, C. E., Malhi, Y., Domingues, L. G., Basso, L. S., Martinewski, A., Correia, C. S. C., Borges, V. F., Freitas, S., Braz, R., Anderson, L. O., Rocha, H., Grace, J., Phillips, O. L., and Lloyd, J.: Drought sensitivity of Amazonian carbon balance revealed by atmospheric measurements, *Nature*, 506, <https://doi.org/10.1038/nature12957>, <http://dx.doi.org/10.1038/nature12957>, 2014.
- Girardin, C. A. J., Malhi, Y., Doughty, C. E., Metcalfe, D. B., Meir, P., del Aguila-Pasquel, J., Araujo-Murakami, A., da Costa, A. C. L., Silva-Espejo, J. E., Farfán Amézquita, F., and Rowland, L.: Seasonal trends of Amazonian rainforest phenology, net primary productivity, and carbon allocation, *Global Biogeochemical Cycles*, 30, 700–715, <https://doi.org/10.1002/2015GB005270>, <https://agupubs.onlinelibrary.wiley.com/doi/abs/10.1002/2015GB005270>, 2016.
- Gloor, E., Wilson, C., Chipperfield, M. P., Chevallier, F., Buermann, W., Boesch, H., Parker, R., Somkuti, P., Gatti, L. V., Correia, C., Domingues, L. G., Peters, W., Miller, J., Deeter, M. N., and Sullivan, M. J. P.: Tropical land carbon cycle responses to 2015/16 El Niño as recorded by atmospheric greenhouse gas and remote sensing data, *Philosophical Transactions of the Royal Society B: Biological Sciences*, 373, 20170302, <https://doi.org/10.1098/rstb.2017.0302>, <https://royalsocietypublishing.org/doi/abs/10.1098/rstb.2017.0302>, 2018.
- Harper, A. B., Cox, P. M., Friedlingstein, P., Wiltshire, A. J., Jones, C. D., Sitch, S., Mercado, L. M., Groenendijk, M., Robertson, E., Kattge, J., Bönisch, G., Atkin, O. K., Bahn, M., Cornelissen, J., Niinemets, U., Onipchenko, V., Peñuelas, J., Poorter, L., Reich, P. B., Soudzilovskaia, N. A., and Bodegom, P. V.: Improved representation of plant functional types and physiology in the Joint UK Land Environment Simulator (JULES v4.2) using plant trait information, *Geoscientific Model Development*, 9, 2415–2440, <https://doi.org/10.5194/gmd-9-2415-2016>, <https://www.geosci-model-dev.net/9/2415/2016/>, 2016.
- Harris, I. C.: CRU JRA v1.1: A forcings dataset of gridded land surface blend of Climatic Research Unit (CRU) and Japanese reanalysis (JRA) data; Jan.1901 - Dec.2017., <https://doi.org/10.5285/13f3635174794bb98cf8ac4b0ee8f4ed>, <http://dx.doi.org/10.5285/13f3635174794bb98cf8ac4b0ee8f4ed>, 2019.
- Hartmann, H. and Trumbore, S.: Understanding the roles of nonstructural carbohydrates in forest trees – from what we can measure to what we want to know, *New Phytologist*, 211, 386–403, <https://doi.org/10.1111/nph.13955>, <http://dx.doi.org/10.1111/nph.13955>, 2016-21190, 2016.
- Hemming, D., Fritts, H., Leavitt, S., Wright, W., Long, A., and Shashkin, A.: Modelling tree-ring $\delta^{13}C$, *Dendrochronologia*, 19, 23–38, 2001.
- Hewitt, A. J., Booth, B. B. B., Jones, C. D., Robertson, E. S., Wiltshire, A. J., Sansom, P. G., Stephenson, D. B., and Yip, S.: Sources of Uncertainty in Future Projections of the Carbon Cycle, *Journal of Climate*, 29, 7203–7213, <https://doi.org/10.1175/JCLI-D-16-0161.1>, <https://doi.org/10.1175/JCLI-D-16-0161.1>, 2016.
- Huntingford, C., Lowe, J. A., Booth, B. B. B., Jones, C. D., Harris, G. R., Gohar, L. K., and Meir, P.: Contributions of carbon cycle uncertainty to future climate projection spread, *Tellus B*, 61, 355–360, <https://doi.org/10.1111/j.1600-0889.2009.00414.x>, <https://onlinelibrary.wiley.com/doi/abs/10.1111/j.1600-0889.2009.00414.x>, 2009.
- Huntingford, C., Zelazowski, P., Galbraith, D., Mercado, L. M., Sitch, S., Fisher, R., Lomas, M., Walker, A. P., Jones, C. D., Booth, B. B. B., Malhi, Y., Hemming, D., Kay, G., Good, P., Lewis, S. L., Phillips, O. L., Atkin, O. K., Lloyd, J., Gloor, E., Zaragoza-Castells, J., Meir, P., Betts, R., Harris, P. P., Nobre, C., Marengo, J., and Cox, P. M.: Simulated resilience of tropical rainforests to CO₂-induced climate change, *Nature Geoscience*, 6, 268–273, <http://dx.doi.org/10.1038/ngeo1741>, 2013.
- IPCC: 2014: Climate Change 2014: Synthesis Report. Contribution of Working Groups I, II and III to the Fifth Assessment Report of the Intergovernmental Panel on Climate Change [Core Writing Team, R.K. Pachauri and L.A. Meyer (eds.)], IPCC, Geneva, Switzerland, 151 pp., 2014.
- Körner, C.: Carbon limitation in trees, *Journal of Ecology*, 91, 4–17, <https://doi.org/10.1046/j.1365-2745.2003.00742.x>, <http://dx.doi.org/10.1046/j.1365-2745.2003.00742.x>, 2003.
- Landhüsser, S. M., Chow, P. S., Dickman, L. T., Furze, M. E., Kuhlman, I., Schmid, S., Wiesenbauer, J., Wild, B., Gleixner, G., Hartmann, H., Hoch, G., McDowell, N. G., Richardson, A. D., Richter, A., and Adams, H. D.: Standardized protocols and procedures can precisely



Simon Jones: A Simple Representation of NSC

15

- and accurately quantify non-structural carbohydrates, *Tree Physiology*, 38, 1764–1778, <https://doi.org/10.1093/treephys/tpy118>, <https://doi.org/10.1093/treephys/tpy118>, 2018.
- Liu, J., Bowman, K. W., Schimel, D. S., Parazoo, N. C., Jiang, Z., Lee, M., Bloom, A. A., Wunch, D., Frankenberg, C., Sun, Y., O'Dell, C. W., Gurney, K. R., Menemenlis, D., Gierach, M., Crisp, D., and Eldering, A.: Contrasting carbon cycle responses of the tropical continents to the 2015–2016 El Niño, *Science*, 358, <https://doi.org/10.1126/science.aam5690>, <https://science.sciencemag.org/content/358/6360/eaam5690>, 2017.
- Lovenduski, N. S. and Bonan, G. B.: Reducing uncertainty in projections of terrestrial carbon uptake, *Environmental Research Letters*, 12, 4, <https://doi.org/10.1088/1748-9326/aa66b8>, 2017.
- Luo, X., Keenan, T. F., Fisher, J. B., Jiménez-Muñoz, J.-C., Chen, J. M., Jiang, C., Ju, W., Perakalapati, N.-V., Ryu, Y., and Tadić, J. M.: The impact of the 2015/2016 El Niño on global photosynthesis using satellite remote sensing, *Philosophical Transactions of the Royal Society B: Biological Sciences*, 373, 20170409, <https://doi.org/10.1098/rstb.2017.0409>, <https://royalsocietypublishing.org/doi/abs/10.1098/rstb.2017.0409>, 2018.
- Marengo, J. A., Souza, C. M., Thonicke, K., Burton, C., Halladay, K., Betts, R. A., Alves, L. M., and Soares, W. R.: Changes in Climate and Land Use Over the Amazon Region: Current and Future Variability and Trends, *Frontiers in Earth Science*, 6, 228, <https://doi.org/10.3389/feart.2018.00228>, <https://www.frontiersin.org/article/10.3389/feart.2018.00228>, 2018.
- Martínez-Vilalta, J., Poyatos, R., Aguadé, D., Retana, J., and Mencuccini, M.: A new look at water transport regulation in plants, *New Phytologist*, 204, 105–115, <https://doi.org/10.1111/nph.12912>, <https://nph.onlinelibrary.wiley.com/doi/abs/10.1111/nph.12912>, 2014.
- Martínez-Vilalta, J., Sala, A., Asensio, D., Galiano, L., Hoch, G., Palacio, S., Piper, F. I., and Lloret, F.: Dynamics of non-structural carbohydrates in terrestrial plants: a global synthesis, *Ecological Monographs*, 86, 495–516, <https://doi.org/10.1002/ecm.1231>, <http://dx.doi.org/10.1002/ecm.1231>, 2016.
- McDowell, N., Pockman, W. T., Allen, C. D., Breshears, D. D., Cobb, N., Kolb, T., Plaut, J., Sperry, J., West, A., Williams, D. G., and Yezpe, E. A.: Mechanisms of plant survival and mortality during drought: why do some plants survive while others succumb to drought?, *New Phytologist*, 178, 719–739, 2008.
- Meir, P., Mencuccini, M., Binks, O., da Costa, A. L., Ferreira, L., and Rowland, L.: Short-term effects of drought on tropical forest do not fully predict impacts of repeated or long-term drought: gas exchange versus growth, *Philosophical Transactions of the Royal Society B: Biological Sciences*, 373, 20170311, <https://doi.org/10.1098/rstb.2017.0311>, <https://royalsocietypublishing.org/doi/abs/10.1098/rstb.2017.0311>, 2018.
- Mencuccini, M., Manzoni, S., and Christoffersen, B.: Modelling water fluxes in plants: from tissues to biosphere, *New Phytologist*, 222, 1207–1222, <https://doi.org/10.1111/nph.15681>, <https://nph.onlinelibrary.wiley.com/doi/abs/10.1111/nph.15681>, 2019.
- Metcalfe, D. B., Meir, P., Aragão, L. E. O. C., Lobo-do Vale, R., Galbraith, D., Fisher, R. A., Chaves, M. M., Maroco, J. P., da Costa, A. C. L., de Almeida, S. S., Braga, A. P., Gonçalves, P. H. L., de Athaydes, J., da Costa, M., Portela, T. T. B., de Oliveira, A. A. R., Malhi, Y., and Williams, M.: Shifts in plant respiration and carbon use efficiency at a large-scale drought experiment in the eastern Amazon, *New Phytologist*, 187, 608–621, <https://doi.org/10.1111/j.1469-8137.2010.03319.x>, <https://nph.onlinelibrary.wiley.com/doi/abs/10.1111/j.1469-8137.2010.03319.x>, 2010.
- Mitchell, P. J., O'Grady, A. P., Tissue, D. T., White, D. A., Ottenschlaeger, M. L., and Pinkard, E. A.: Drought response strategies define the relative contributions of hydraulic dysfunction and carbohydrate depletion during tree mortality, *New Phytologist*, 197, 862–872, <https://doi.org/10.1111/nph.12064>, <https://nph.onlinelibrary.wiley.com/doi/abs/10.1111/nph.12064>, 2013.
- Muller, B., Pantin, F., Génard, M., Turc, O., Freixes, S., Piques, M., and Gibon, Y.: Water deficits uncouple growth from photosynthesis, increase C content, and modify the relationships between C and growth in sink organs, *Journal of Experimental Botany*, 62, 1715–1729, <https://doi.org/10.1093/jxb/erq438>, <https://doi.org/10.1093/jxb/erq438>, 2011.
- O'Brien, M. J., Leuzinger, S., Philipson, C. D., Tay, J., and Hector, A.: Drought survival of tropical tree seedlings enhanced by non-structural carbohydrate levels, *Nature Climate Change*, 4, 710–714, <https://doi.org/10.1038/nclimate2281>, <https://doi.org/10.1038/nclimate2281>, 2014.
- Palacio, S., Hoch, G., Sala, A., Körner, C., and Millard, P.: Does carbon storage limit tree growth?, *New Phytologist*, 201, 1096–1100, <https://doi.org/10.1111/nph.12602>, <http://dx.doi.org/10.1111/nph.12602>, 2013-16122, 2014.
- Pan, Y., Birdsey, R. A., Fang, J., Houghton, R., Kauppi, P. E., Kurz, W. A., Phillips, O. L., Shvidenko, A., Lewis, S. L., Canadell, J. G., Ciais, P., Jackson, R. B., Pacala, S. W., McGuire, A. D., Piao, S., Rautiainen, A., Sitch, S., and Hayes, D.: A Large and Persistent Carbon Sink in the World's Forests, *Science*, 333, 988–993, <https://doi.org/10.1126/science.1201609>, <https://science.sciencemag.org/content/333/6045/988>, 2011.
- Parazoo, N. C., Bowman, K., Fisher, J. B., Frankenberg, C., Jones, D. B. A., Cescatti, A., Pérez-Priego, O., Wohlfahrt, G., and Montagnani, L.: Terrestrial gross primary production inferred from satellite fluorescence and vegetation models, *Global Change Biology*, 20, 3103–3121, <https://doi.org/10.1111/gcb.12652>, <https://onlinelibrary.wiley.com/doi/abs/10.1111/gcb.12652>, 2014.
- Phillips, O. L., Aragão, L. E. O. C., Lewis, S. L., Fisher, J. B., Lloyd, J., López-González, G., Malhi, Y., Monteagudo, A., Peacock, J., Quesada, C. A., van der Heijden, G., Almeida, S., Amaral, I., Arroyo, L., Aymard, G., Baker, T. R., Bánki, O., Blanc, L., Bonal, D., Brando, P., Chave, J., de Oliveira, Á. C. A., Cardozo, N. D., Czimeczik, C. I., Feldpausch, T. R., Freitas, M. A., Gloor, E., Higuchi, N., Jiménez, E., Lloyd, G., Meir, P., Mendoza, C., Morel, A., Neill, D. A., Nepstad, D., Patiño, S., Peñuela, M. C., Prieto, A., Ramírez, F., Schwarz, M., Silva, J., Silveira, M., Thomas, A. S., Steege, H. t., Stropp, J., Vázquez, R., Zelazowski, P., Dávila, E. A., Andelman, S., Andrade, A., Chao, K.-J., Erwin, T., Di Fiore, A. C., E. H., Keeling, H., Killeen, T. J., Laurance, W. F., Cruz, A. P., Pitman, N. C. A., Vargas, P. N., Ramírez-



- Angulo, H., Rudas, A., Salamão, R., Silva, N., Terborgh, J., and Torres-Lezama, A.: Drought Sensitivity of the Amazon Rainforest, *Science*, 323, 1344–1347, <https://doi.org/10.1126/science.1164033>, <https://science.sciencemag.org/content/323/5919/1344>, 2009.
- Poulter, B., Frank, D., Ciais, P., Myneni, R. B., Andela, N., Bi, J., Broquet, G., Canadell, J. G., Chevallier, F., Liu, Y. Y., Running, S. W., Sitch, S., and van der Werf, G. R.: Contribution of semi-arid ecosystems to interannual variability of the global carbon cycle, *Nature*, 509, <https://doi.org/10.1038/nature13376>, <https://doi.org/10.1038/nature13376>, 2014.
- Powell, T. L., Galbraith, D. R., Christoffersen, B. O., Harper, A., Imbuzeiro, H. M. A., Rowland, L., Almeida, S., Brando, P. M., Costa, A. C. L., Costa, M. H., Levine, N. M., Malhi, Y., Saleska, S. R., Sotta, E., Williams, M., Meir, P., and Moorcroft, P. R.: Confronting model predictions of carbon fluxes with measurements of Amazon forests subjected to experimental drought, *New Phytologist*, 200, 350–365, <https://doi.org/10.1111/nph.12390>, <https://nph.onlinelibrary.wiley.com/doi/abs/10.1111/nph.12390>, 2013.
- Quentin, A. G., Pinkard, E. A., Ryan, M. G., Tissue, D. T., Baggett, L. S., Adams, H. D., Maillard, P., Marchand, J., Landhäusser, S. M., Lacointe, A., Gibon, Y., Anderegg, W. R., Asao, S., Atkin, O. K., Bonhomme, M., Claye, C., Chow, P. S., Clément-Vidal, A., Davies, N. W., Dickman, L. T., Dumbur, R., Ellsworth, D. S., Falk, K., Galiano, L., Grünzweig, J. M., Hartmann, H., Hoch, G., Hood, S., Jones, J. E., Koike, T., Kuhlmann, I., Lloret, F., Maestro, M., Mansfield, S. D., Martínez-Vilalta, J., Maucourt, M., McDowell, N. G., Moing, A., Muller, B., Nebauer, S. G., Niinemets, U., Palacio, S., Piper, F., Raveh, E., Richter, A., Rolland, G., Rosas, T., Saint Joanis, B., Sala, A., Smith, R. A., Sterck, F., Stinziano, J. R., Tobias, M., Unda, F., Watanabe, M., Way, D. A., Weerasinghe, L. K., Wild, B., Wiley, E., and Woodruff, D. R.: Non-structural carbohydrates in woody plants compared among laboratories, *Tree Physiology*, 35, 1146–1165, <https://doi.org/10.1093/treephys/tpv073>, <https://doi.org/10.1093/treephys/tpv073>, 2015.
- Rowland, L., da Costa, A. C. L., Galbraith, D. R., Oliveira, R. S., Binks, O. J., Oliveira, A. A. R., Pullen, A. M., Doughty, C. E., Metcalfe, D. B., Vasconcelos, S. S., Ferreira, L. V., Malhi, Y., Grace, J., Mencuccini, M., and Meir, P.: Death from drought in tropical forests is triggered by hydraulics not carbon starvation, *Nature*, 528, <https://doi.org/10.1038/nature15539>, <https://doi.org/10.1038/nature15539>, 2015.
- Rowland, L., da Costa, A. C. L., Oliveira, A. A. R., Almeida, S. S., Ferreira, L. V., Malhi, Y., Metcalfe, D. B., Mencuccini, M., Grace, J., and Meir, P.: Shock and stabilisation following long-term drought in tropical forest from 15 years of litterfall dynamics, *Journal of Ecology*, 106, 1673–1682, <https://doi.org/10.1111/1365-2745.12931>, <https://besjournals.onlinelibrary.wiley.com/doi/abs/10.1111/1365-2745.12931>, 2018.
- Roxburgh, S. H., Berry, S. L., Buckley, T. N., Barnes, B., and Roderick, M. L.: What is NPP? Inconsistent accounting of respiratory fluxes in the definition of net primary production, *Functional Ecology*, 19, 378–382, <https://doi.org/10.1111/j.1365-2435.2005.00983.x>, <https://besjournals.onlinelibrary.wiley.com/doi/abs/10.1111/j.1365-2435.2005.00983.x>, 2005.
- Sala, A. and Mencuccini, M.: Plump trees win under drought, *Nature Climate Change*, 4, 666–667, <https://doi.org/10.1038/nclimate2329>, <https://doi.org/10.1038/nclimate2329>, 2014.
- Salomón, R. L., De Roo, L., Oleksyn, J., De Pauw, D. J. W., and Steppe, K.: TReSpire – a biophysical TRee Stem respiration model, *New Phytologist*, n/a, <https://doi.org/10.1111/nph.16174>, <https://nph.onlinelibrary.wiley.com/doi/abs/10.1111/nph.16174>, 2019.
- Sevanto, S., McDowell, N. G., Dickman, L. T., Pangle, R., and Pockman, W. T.: How do trees die? A test of the hydraulic failure and carbon starvation hypotheses, *Plant, Cell & Environment*, 37, 153–161, <https://doi.org/10.1111/pce.12141>, <https://onlinelibrary.wiley.com/doi/abs/10.1111/pce.12141>, 2014.
- Sitch, S., Huntingford, C., Gedney, N., Levy, P. E., Lomas, M., Piao, S. L., Betts, R., Ciais, P., Cox, P., Friedlingstein, P., Jones, C. D., Prentice, I. C., and Woodward, F. I.: Evaluation of the terrestrial carbon cycle, future plant geography and climate-carbon cycle feedbacks using five Dynamic Global Vegetation Models (DGVMs), *Global Change Biology*, 14, 2015–2039, <https://doi.org/10.1111/j.1365-2486.2008.01626.x>, <https://onlinelibrary.wiley.com/doi/abs/10.1111/j.1365-2486.2008.01626.x>, 2008.
- Sperry, J. S. and Love, D. M.: What plant hydraulics can tell us about responses to climate-change droughts, *New Phytologist*, 207, 14–27, <https://doi.org/10.1111/nph.13354>, <https://nph.onlinelibrary.wiley.com/doi/abs/10.1111/nph.13354>, 2015.
- Sperry, J. S., Venturas, M. D., Anderegg, W. R. L., Mencuccini, M., Mackay, D. S., Wang, Y., and Love, D. M.: Predicting stomatal responses to the environment from the optimization of photosynthetic gain and hydraulic cost, *Plant, Cell & Environment*, 40, 816–830, <https://doi.org/10.1111/pce.12852>, <https://onlinelibrary.wiley.com/doi/abs/10.1111/pce.12852>, 2017.
- Stitt, M.: Rising CO₂ levels and their potential significance for carbon flow in photosynthetic cells, *Plant, Cell & Environment*, 14, 741–762, <https://doi.org/10.1111/j.1365-3040.1991.tb01440.x>, <https://onlinelibrary.wiley.com/doi/abs/10.1111/j.1365-3040.1991.tb01440.x>, 1991.
- Thornley, J. and Cannell, M.: Modelling the Components of Plant Respiration: Representation and Realism, *Annals of Botany*, 85, 55 – 67, <https://doi.org/https://doi.org/10.1006/anbo.1999.0997>, <http://www.sciencedirect.com/science/article/pii/S0305736499909976>, 2000.
- Thornley, J. H. M.: Respiration, Growth and Maintenance in Plants, *Nature*, 227, 304–305, <https://doi.org/10.1038/227304b0>, <https://doi.org/10.1038/227304b0>, 1970.
- Thornley, J. H. M.: Energy, Respiration, and Growth in Plants, *Annals of Botany*, 35, 721–728, <https://doi.org/10.1093/oxfordjournals.aob.a084519>, <https://doi.org/10.1093/oxfordjournals.aob.a084519>, 1971.
- Thornley, J. H. M.: A Model to Describe the Partitioning of Photosynthate during Vegetative Plant Growth, *Annals of Botany*, 36, 419–430, <https://doi.org/10.1093/oxfordjournals.aob.a084601>, <https://doi.org/10.1093/oxfordjournals.aob.a084601>, 1972a.
- Thornley, J. H. M.: A Balanced Quantitative Model for Root: Shoot Ratios in Vegetative Plants, *Annals of Botany*, 36, 431–441, <https://doi.org/10.1093/oxfordjournals.aob.a084602>, <https://doi.org/10.1093/oxfordjournals.aob.a084602>, 1972b.
- Thornley, J. H. M.: Growth, Maintenance and Respiration: a Re-interpretation, *Annals of Botany*, 41, 1191–1203, <https://doi.org/10.1093/oxfordjournals.aob.a085409>, <https://doi.org/10.1093/oxfordjournals.aob.a085409>, 1977.



Simon Jones: A Simple Representation of NSC

17

- Thornley, J. H. M.: A Transport-resistance Model of Forest Growth and Partitioning, *Annals of Botany*, 68, 211–226, <https://doi.org/10.1093/oxfordjournals.aob.a088246>, <https://doi.org/10.1093/oxfordjournals.aob.a088246>, 1991.
- Thornley, J. H. M.: Modelling allocation with transport/conversion processes, *Silva Fennica*, 31, 341–355, <https://doi.org/10.14214/sf.a8532>, 1997.
- Thornley, J. H. M.: Plant growth and respiration re-visited: maintenance respiration defined -it is an emergent property of, not a separate process within, the system - and why the respiration : photosynthesis ratio is conservative, *Annals of Botany*, 108, 1365–1380, <https://doi.org/10.1093/aob/mcr238>, <https://doi.org/10.1093/aob/mcr238>, 2011.
- Thornley, J. H. M. and Johnson, I. R.: *Plant and Crop Modelling. A Mathematical Approach to Plant and Crop Physiology*, The Blackburn Press, 1990.
- Trugman, A. T., Detto, M., Bartlett, M. K., Medvigy, D., Anderegg, W. R. L., Schwalm, C., Schaffer, B., and Pacala, S. W.: Tree carbon allocation explains forest drought-kill and recovery patterns, *Ecology Letters*, 21, 1552–1560, <https://doi.org/10.1111/ele.13136>, <https://onlinelibrary.wiley.com/doi/abs/10.1111/ele.13136>, 2018.
- Tyree, M. T. and Sperry, J. S.: Vulnerability of Xylem to Cavitation and Embolism, *Annual Review of Plant Physiology and Plant Molecular Biology*, 40, 19–36, <https://doi.org/10.1146/annurev.pp.40.060189.000315>, <https://doi.org/10.1146/annurev.pp.40.060189.000315>, 1989.
- UN Food and Agriculture Organization Rome: *Global Forest Resources Assessment*, <http://www.fao.org/3/a-i4808e.pdf>, 2015.
- Wiley, E. and Helliker, B.: A re-evaluation of carbon storage in trees lends greater support for carbon limitation to growth, *New Phytologist*, 195, 285–289, <https://doi.org/10.1111/j.1469-8137.2012.04180.x>, <http://dx.doi.org/10.1111/j.1469-8137.2012.04180.x>, 2012.
- Williams, K. E., Harper, A. B., Huntingford, C., Mercado, L. M., Mathison, C. T., Falloon, P. D., Cox, P. M., and Kim, J.: Revisiting the First ISLSCP Field Experiment to evaluate water stress in JULESv5.0, *Geoscientific Model Development Discussions*, pp. 1–47, <https://doi.org/10.5194/gmd-2018-210>, <https://app.dimensions.ai/details/publication/pub.1107298487> and <https://www.geosci-model-dev-discuss.net/gmd-2018-210/gmd-2018-210.pdf>, 2018.
- Würth, M. K. R., Peláez-Riedl, S., Wright, S. J., and Körner, C.: Non-structural carbohydrate pools in a tropical forest, *Oecologia*, 143, 11–24, <https://doi.org/10.1007/s00442-004-1773-2>, <https://doi.org/10.1007/s00442-004-1773-2>, 2005.

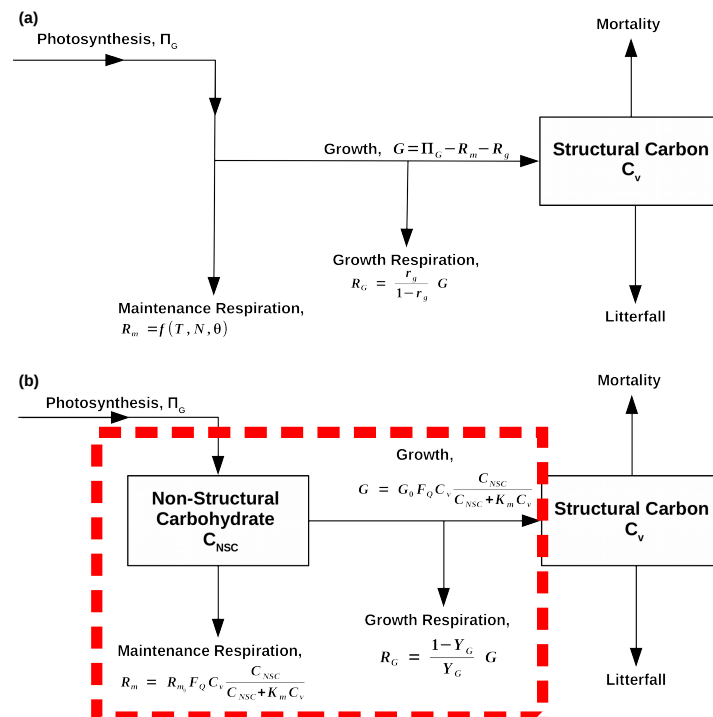


Figure 1. Flow diagrams that demonstrate how SUGAR is designed to change the model structure of carbon allocation within the Joint UK Land Environment Simulator (JULES) (Best et al., 2011; Clark et al., 2011)). Arrows represent fluxes of carbon and black boxes represent carbon pools. **(a)** A representation of the current structure of carbon allocation in JULES. Maintenance respiration (R_m) depends on temperature (T), leaf nitrogen (N) and optionally, water availability (θ). Growth respiration (R_G) is equal to a constant fraction of growth (G) which is equal to photosynthesis (Π_G) less total plant respiration ($R_G + R_m$). Total utilisation of carbon ($R_m + R_G + G$) is always exactly equal to carbon assimilation by photosynthesis (Π_G). **(b)** A representation of how SUGAR would sit within JULES. The red dashed box represents the model boundary of SUGAR. Both maintenance respiration and growth depend on temperature via a Q_{10} function (F_Q), structural biomass (C_v) and non-structural carbohydrate content (C_{NSC}). Growth respiration is a constant fraction of growth.

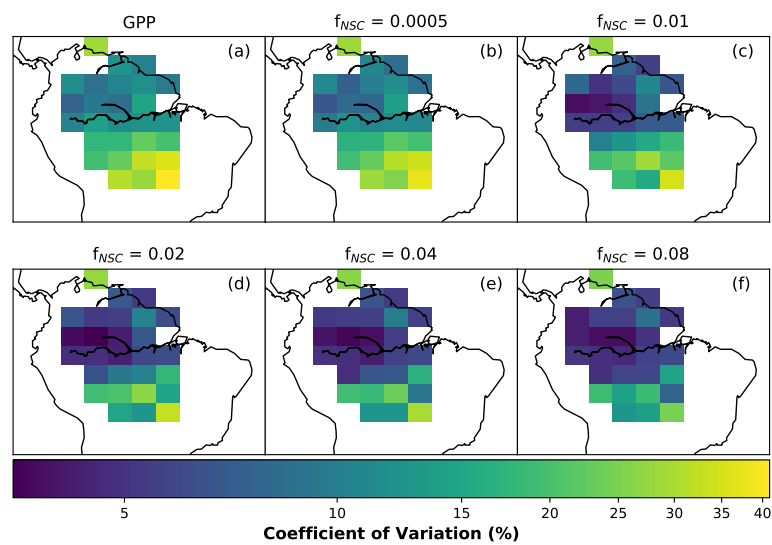


Figure 2. The coefficient of variation of (a) GPP (Parazoo et al., 2014) and (b-f) simulated Plant Carbon Expenditure (PCE) for different initialised carbohydrate content as a fraction of grid-box Biomass (f_{NSC}).

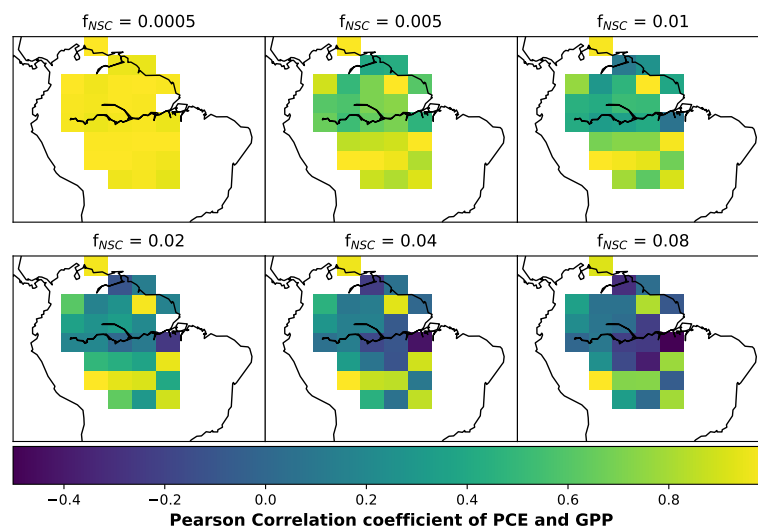


Figure 3. The Pearson correlation coefficient of simulated plant carbon expenditure (PCE) and driving gross primary productivity (GPP) for different initialised carbohydrate contents as a fraction (f_{NSC}) of grid-box biomass. This gives an indication of how important a driver GPP is for PCE in each grid-box.

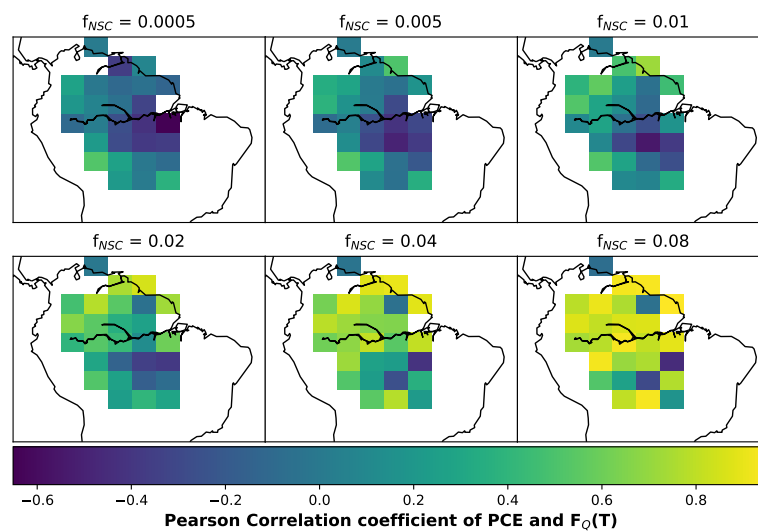


Figure 4. The Pearson correlation coefficient of simulated plant carbon expenditure (PCE) and driving Q_{10} (F_Q) for different initialised carbohydrate contents as a fraction (f_{NSC}) of grid-box biomass. This gives an indication of how important a driver the Q_{10} function is for PCE in each grid-box.

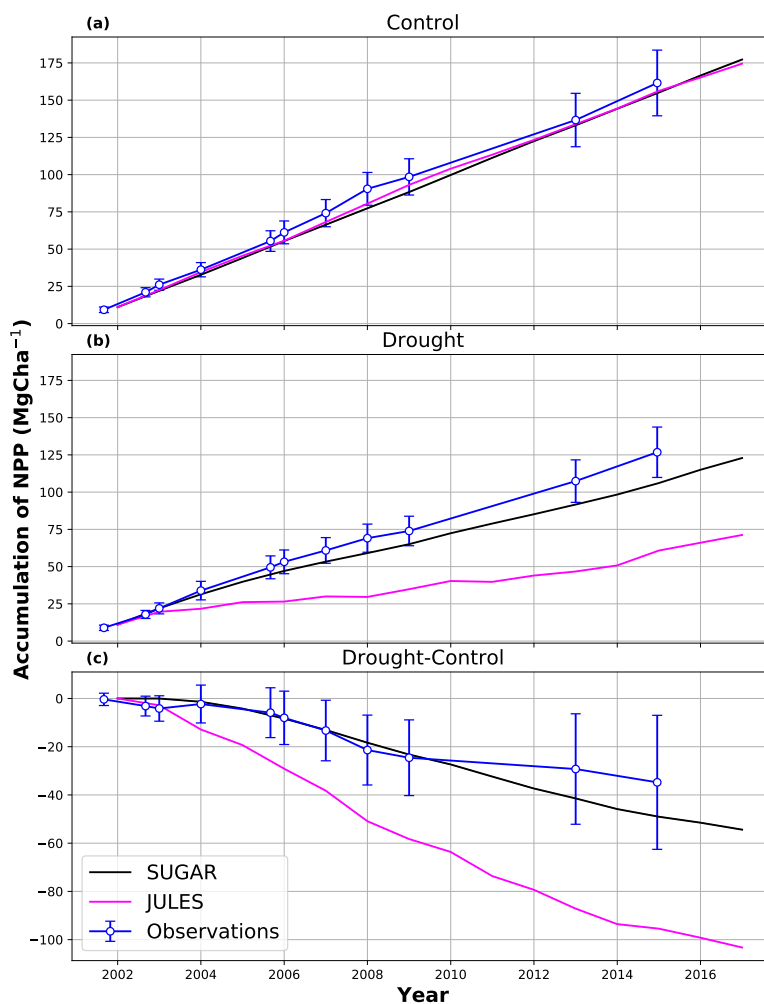


Figure 5. Accumulated Net Primary Productivity at Caxiuanã in (a) Control plot, (b) TFE plot and (c) The difference between the drought and control forest (TFE-control). Observations are calculated as the accumulated sum of biomass increment change and local litter-fall (Rowland et al., 2018). The presented confidence intervals are the sum of the litterfall measurement error and the 95% confidence intervals of biomass increment calculated from 8 allometric equations using trunk diameter at breast height (DBH) data from Caxiuanã.

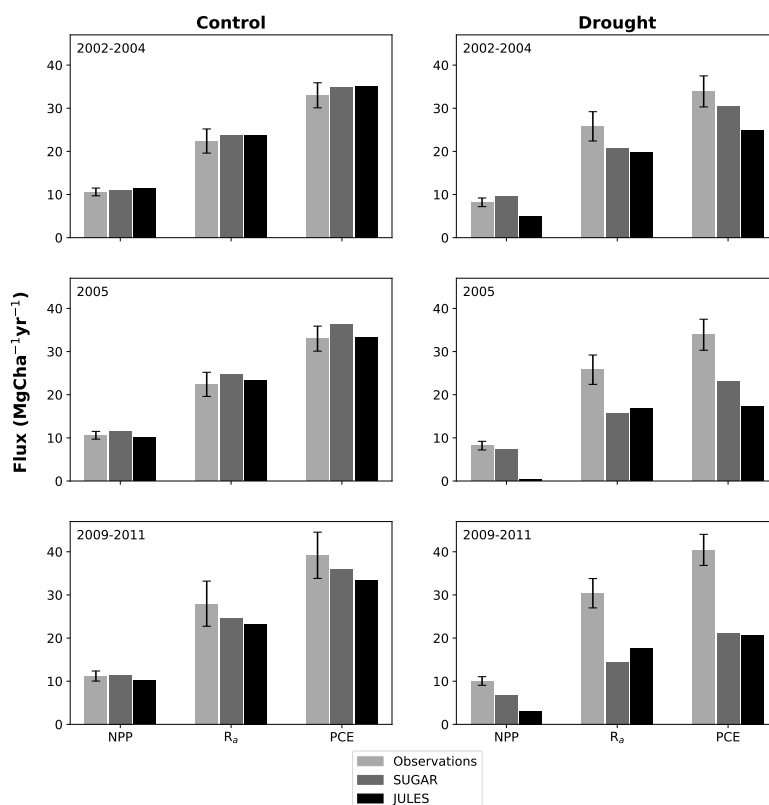


Figure 6. Net primary productivity (NPP), Autotrophic respiration (R_p) and Plant Carbon Expenditure ($PCE = NPP + R_p$); for the periods 2002-2004, 2005 and 2009-2011. The left column is from the control plot and the right is from the through-fall exclusion (TFE) plot. Model predictions from JULES and SUGAR are calculated by taking the mean of each flux over each period. Observations for 2005 are from Metcalfe et al. (2010) and observations from 2009-2011 are from da Costa et al. (2014). Simulated photosynthesis in JULES responded almost instantly to the introduction of the panels on the TFE plot which meant that NPP, R_p and PCE changed significantly in both models between 2002 and 2005. To demonstrate this change we show predicted fluxes during the 2002-2004 period as well as from 2005. Observations for this period are not available to such a comprehensive degree as they are for 2005 and the 2009-2011 period. For this reason we compare the model predictions for 2002-2004 to the 2005 observations. This is reasonable in the control plot where it is plausible that the forest was in steady state (Metcalfe et al., 2010) and so fluxes from 2005 will be similar to those during the 2002-2004 period. In the TFE plot while there were some significant changes in observed carbon fluxes during the first 3 years of the experiment, (for example the production of leaves, flowers and fruits, and fine wood (Rowland et al., 2018; Meir et al., 2018)), the forest largely resisted the effects of the drought during this period (significant increases in mortality were not seen until 2005 (Rowland et al., 2015; Meir et al., 2018)) and so we can similarly expect fluxes from 2002-2004 to be comparable to those from 2005. Nonetheless, care should be taken with these comparisons in both plots.

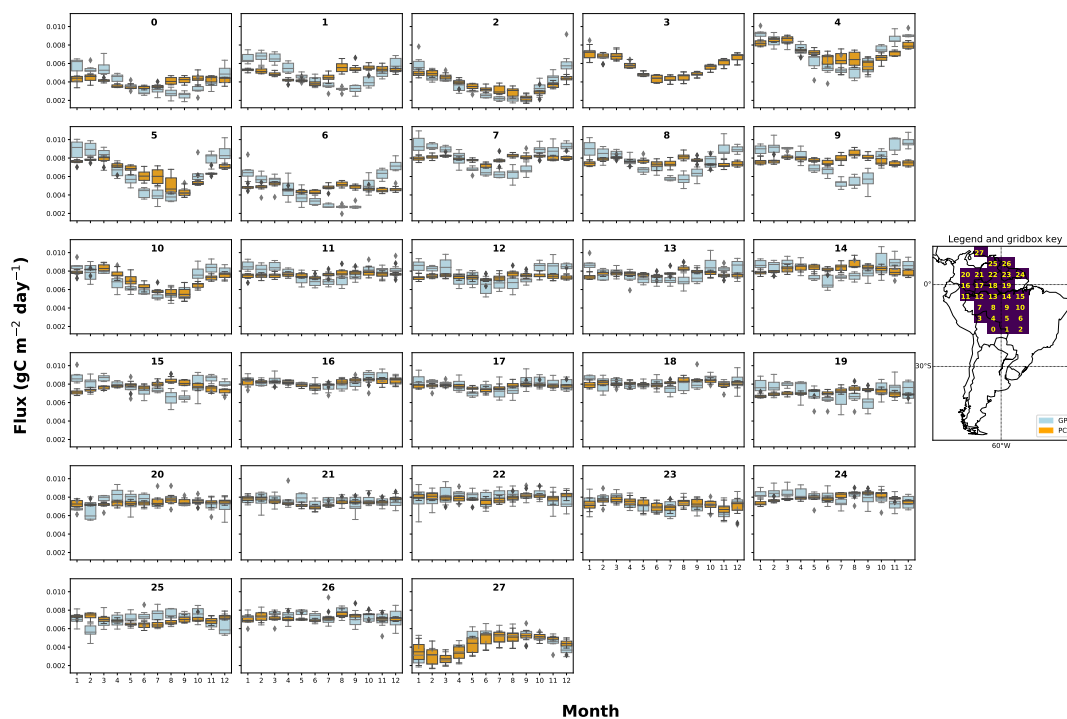


Figure A1. The mean seasonal trend of simulated plant carbon expenditure (PCE) and forcing gross primary productivity (GPP) (Parazoo et al., 2014) for each gridbox in the $f_{NSC} = 0.08$ SUGAR simulations. The map key shows which plot corresponds to which grid-box.



Symbol	Units	Definition
a_{K_m}		Saturation parameter
C_{NSC}	kg C m^{-2}	NSC content
C_v	kg C m^{-2}	Structural carbon content
f_{NSC}		Equilibrium NSC mass fraction
F_Q		Q_{10} function for growth and respiration
G	$\text{kg C m}^{-2} \text{ s}^{-1}$	Plant growth
G_0	s^{-1}	Specific growth rate
q_{10}		Q_{10} value for plant respiration and growth
R_g	$\text{kg C m}^{-2} \text{ s}^{-1}$	Growth respiration
R_m	$\text{kg C m}^{-2} \text{ s}^{-1}$	Maintenance respiration
R_{m_0}	s^{-1}	Specific rate of maintenance respiration
R_p	$\text{kg C m}^{-2} \text{ s}^{-1}$	Total plant respiration
T	$^{\circ}\text{C}$	Temperature
U	$\text{kg C m}^{-2} \text{ s}^{-1}$	Plant carbon expenditure
Y_g		Growth yield coefficient
α		Ratio of plant growth to PCE
Π	$\text{kg C m}^{-2} \text{ s}^{-1}$	Net primary productivity
Π_G	$\text{kg C m}^{-2} \text{ s}^{-1}$	Gross primary productivity
τ	s	Ecosystem carbon residency time
ϕ	s^{-1}	Specific rate of carbohydrate utilisation

Table 1. Definitions of Symbols



Author	Equation	a	b	c	d	E
Brown 97a	$a + bD + cD^2$	42.69	-12.8	1.242		
Brown 97b	$\exp(a + b\log_e(D))$	-2.134	2.53			
Carvalho 98	$1000a\exp(b + c\log_e(D/100))$	0.6	3.323	2.546		
Araujo 99	abD^c	0.6	4.06	1.76		
Chambers 01	$\exp(a + b\log_e(D) + c\log_e(D)^2 + d\log(D)^3)$	-0.37	0.333	0.933	-0.122	
Baker 04	$\exp(a + b\log_e(D) + c\log_e(D)^2 + d\log(D)^3)(\rho/0.67)$	-0.37	0.333	0.933	-0.122	
Chave 05	$\exp(a + b\log_e(D) + c\log_e(D)^2 + d\log(D)^3)(\rho)$	-1.499	2.148	0.207	-0.0281	
Chave 14	$\exp(a - 0.976E + b\log_e(D) + c\log_e(D)^2 + d\log(\rho))$	-1.803	2.673	-0.0299	0.976	-0.0510307

D = Diameter at breast height (dbh); ρ = Wood density; a, b, c, d, E are constants.

Table 2. Allometric equations used to calculate above-ground biomass, C_v (kg)